Metrologia

On decay constants and orbital distance to the Sun—part I: alpha decay

OPEN ACCESS
IOP Publishing | Bureau International des Poids et Mesures Metrologia
Metrologia **54** (2017) 1–18 doi:10.1088/1681-7575/54/1/1

On decay constants and orbital distance to the Sun—part I: alpha decay

S Pommé[1], H Stroh[1], J Paepen[1], R Van Ammel[1], M Marouli[1], T Altzitzoglou[1], M Hult[1], K Kossert[2], O Nähle[2], H Schrader[2], F Juget[3], C Bailat[3], Y Nedjadi[3], F Bochud[3], T Buchillier[3], C Michotte[4], S Courte[4], M W van Rooy[5], M J van Staden[5], J Lubbe[5], B R S Simpson[5], A Fazio[6], P De Felice[6], T W Jackson[7], W M Van Wyngaardt[7], M I Reinhard[7], J Golya[7], S Bourke[7], T Roy[8], R Galea[8], J D Keightley[9], K M Ferreira[9], S M Collins[9], A Ceccatelli[10], L Verheyen[11], M Bruggeman[11], B Vodenik[12], M Korun[12], V Chisté[13] and M-N Amiot[13]

[1] European Commission, Joint Research Centre (JRC), Directorate for Nuclear Safety and Security, Retieseweg 111, B-2440 Geel, Belgium
[2] Physikalisch-Technische Bundesanstalt (PTB), Bundesallee 100, 38116 Braunschweig, Germany
[3] Institut de Radiophysique, Lausanne (IRA), Switzerland
[4] Bureau International des Poids et Mesures (BIPM), Pavillon de Breteuil, 92310 Sèvres, France
[5] Radioactivity Standards Laboratory (NMISA), 15 Lower Hope Road, Rosebank 7700, Cape Town, South Africa
[6] National Institute of Ionizing Radiation Metrology (ENEA), Casaccia Research Centre, Via Anguillarese, 301—S.M. Galeria I-00060 Roma, C.P. 2400, I-00100 Roma AD, Italy
[7] Australian Nuclear Science and Technology Organisation (ANSTO), Locked Bag 2001, Kirrawee, NSW 2232, Australia
[8] National Research Council of Canada (NRC),1200 Montreal Road, Ottawa, ON, K1A0R6, Canada
[9] National Physical Laboratory (NPL), Hampton Road, Teddington, Middlesex TW11 OLW, UK
[10] Terrestrial Environment Laboratory, IAEA Environment Laboratories, Department of Nuclear Sciences and Applications, International Atomic Energy Agency (IAEA), Vienna International Centre, PO Box 100, 1400 Vienna, Austria
[11] Belgian Nuclear Research Centre (SCK•CEN), Boeretang 200, B-2400 Mol, Belgium
[12] Jožef Stefan Institute (JSI), Jamova 39, 1000 Ljubljana, Slovenia
[13] CEA, LIST, Laboratoire National Henri Becquerel (LNHB), Bât. 602 PC 111, CEA-Saclay, 91191 Gif-sur-Yvette cedex, France

E-mail: stefaan.pomme@ec.europa.eu

Received 21 September 2016, revised 24 October 2016
Accepted for publication 1 November 2016
Published 28 November 2016

Abstract

Claims that proximity to the Sun causes variation of decay constants at permille level have been investigated for alpha decaying nuclides. Repeated decay rate measurements of ^{209}Po, ^{226}Ra, ^{228}Th, ^{230}U, and ^{241}Am sources were performed over periods of 200 d up to two decades at various nuclear metrology institutes around the globe. Residuals from the exponential decay curves were inspected for annual oscillations. Systematic deviations from a purely exponential decay curve differ in amplitude and phase from one data set to another and appear attributable to instabilities in the instrumentation and measurement conditions. The most stable activity measurements of α decaying sources set an upper limit between 0.0006% and 0.006% to the amplitude of annual oscillations in the decay rate. There are no apparent indications for systematic oscillations at a level of weeks or months. Oscillations in phase with Earth's orbital distance to the sun could not be observed within 10^{-5}–10^{-6} range precision.

Keywords: half-life, decay constant, non-exponential decay, radioactivity, Sun, neutrino

(Some figures may appear in colour only in the online journal)

1. Introduction

The exponential decay of radionuclides as a function of time is a cornerstone of nuclear physics and radionuclide metrology [1, 2]. Decay constants for spontaneous radioactive decay are considered invariable in time and space [3, 4]. This convenient trait allows projecting activity values to a point of time in the past as well as into the future. The statistical laws ruling the temporal behaviour of a decay series [5, 6] are even applied for accurate dating in archaeology [7], geo- and cosmochronology [8], nuclear forensics [9], monitoring of nuclear events [10, 11], or age dating of radiopharmaceuticals [11]. Significant violations of the invariability of decay constants would compromise the accuracy by which one can compare activity measurements or even define a reference for the SI-unit becquerel. There would be a natural limit to the precision by which a half-life value can be assigned to a radionuclide, unless conditions could be specified for which an attained value applies.

The premise of invariability of the decay constants of radionuclides decaying by α, β^- and β^+ emission has withstood many experimental tests, showing independence to physical and chemical conditions such as temperature, pressure, and material surroundings [3, 4]. Internal conversion and electron capture (EC) decays are considered to be in a separate category, since the direct involvement of atomic electrons could in principle be affected by the ionisation state and chemical environment, particularly for low-Z nuclides like ^{7}Be, but the magnitude of these effects are still debated [12–14]. Half-life measurements of radionuclides performed over a century in different laboratories show occasional discrepancies [15] which are generally ascribed to incomplete uncertainty assessment [2]. In the last decades, more attention is paid to precision, uncertainty evaluation, and documentation, which is resulting in a growing convergence of published half-life values at a sub-permille level [16].

In 2009, controversy arose due to claims by Jenkins *et al* that seasonal effects at a level of 10^{-3} in repeated decay rate measurements of ^{32}Si/^{36}Cl and ^{226}Ra were due to an annual modulation of the decay constants rather than instabilities in the detection system [17, 18]. Fischbach *et al* postulated a causal correlation with the orbital Earth–Sun distance, possibly through interactions with solar neutrinos or a scalar field affecting the terrestrial fine structure constant [19]. They found support for the neutrino theory by a perturbation of measured ^{54}Mn decay rates coinciding with a solar flare [20] and solar storms [21]. Jenkins *et al* collected experimental evidence of time-dependent decay rates for ^{3}H, ^{22}Na/^{44}Ti, ^{36}Cl, ^{54}Mn, ^{56}Mn, ^{60}Co, ^{85}Kr, ^{90}Sr/^{90}Y, ^{108m}Ag, ^{133}Ba, ^{137}Cs, ^{152}Eu, ^{154}Eu, ^{222}Rn, ^{226}Ra and ^{239}Pu, in which the most often cited periodicity was 1 a, but also cycles of 1 d, 2 a, 11.7 a to 13.5 a were found by means of a time-frequency analysis [22]. Parkhomov [23] found 7 data sets of beta-decaying radionuclides exhibiting periodic variations with a period of 1 year. Influence by the chemical environment was put back on the table when reports claimed changes at a 10^{-2} level in α, β^- and β^+ and EC decay constants depending on temperature and conductivity of the hosting material (see references in [24, 25]). Theoretical considerations predict an influence of the electron environment on α decay, leading to significantly shorter half-lives at high matter densities (up to 10% at 10^4 g cm^{-3} in a high-Z matrix) [25] which has implications for cosmochronology.

As much as these claims attract interest as inspiration for new physical theories or hope for revolutionising cosmic neutrino detection and radioactive waste management [26–28], if true they would have major implications on traceability and equivalence in the common measurement system of radioactive substances. Primary standardisation of activity concentration of a radionuclide in solution [29, 30] is performed down to an accuracy of typically 0.1% [31], and international equivalence is established through key comparisons organised under the auspices of the BIPM [32]. Through the International Reference System (SIR) [33] standardisations performed over half a century worldwide can be compared. Whereas the key comparison data sets may show signs of slight inconsistency [34, 35], there are reasons to assume that these are mainly caused by imperfections in the uncertainty assessments [31, 36, 37] rather than variability in the decay constants. Oscillations of the order of 10^{-3} in primary standardisations would not easily go unnoticed at this level of accuracy, and are therefore unlikely to have occurred.

In the last decade, new experimental evidence has been presented refuting the variability claims of the decay constants. Stability within a level of $<10^{-4}$ at annual time scale was observed in the decay of ^{22}Na/^{44}Ti, ^{108m}Ag, ^{121m}Sn, ^{133}Ba, ^{241}Am [38], ^{137}Cs [39], ^{36}Cl [40], ^{40}K, ^{232}Th [41], ^{226}Ra [42], and ^{90}Sr/^{90}Y [43]. Repeated half-life measurements of short-lived nuclides including ^{44}Sc [44], ^{198}Au [45, 46], ^{222}Rn [47], and daughter nuclides of ^{225}Ac [48, 49] showed consistency over different periods in the year. No significant deviation of ^{40}K, ^{137}Cs, ^{232}Th decay rates could be observed during the occurrence of the strongest solar flares in 2011 and 2012 [50]. The ^{198}Au half-life is identical in a gold wire and sphere, showing independence of the internally generated neutrino flux of ~10^{11} s^{-1} through the surface of the sphere and ~10^{10} s^{-1} of the wire [51]. No evidence could be found for an anti-neutrino flux of 5×10^{10} cm^2 s^{-1} from a reactor influencing the decay of ^{22}Na (EC, β^+) and ^{54}Mn (EC) [52]. Even in the presence of a 3×10^{12} cm^2 s^{-1} reactor antineutrino flux, the measured differences in decay rates of ^{22}Na, ^{54}Mn and ^{60}Co (β^-) sources are only in the 10^{-5} range [53]. Geo- and cosmochronology does not provide any support for heliocentrically variable decay rates in meteorites for ^{36}Cl, ^{40}Ar, ^{87}Rb, ^{147}Sm and ^{235,238}U [54], and neither does the power of a ^{238}Pu source in the Cassini spacecraft show dependence on neutrino

flux through proximity to the Sun [55, 56]. The half-lives of ^{198}Au in gold and ^{97}Ru in ruthenium proved to be the same within 0.04% and <0.1%, respectively, between room temperature and 19 K [24]. A ^{210}Po source imbedded in silver showed the expected decay rate within 0.6% after having been cooled down to 4.2 K for 28 d [57], which is incompatible with a claim that the decay constant would reduce by 6.3% in these conditions.

In summary, the anomalies in the ^{36}Cl and ^{226}Ra decays have been disproved with new, more stable measurements and additional evidence demonstrates the invariability of various decay constants under different physical and chemical constraints. Nevertheless, arguments were raised that the variability may differ from one nuclide to another and that experimental proof for a variety of nuclides and a variety of detectors is needed [17, 22]. In this work, 14 radionuclide metrology laboratories from across the globe present repeated activity measurements of various mono-radionuclide sources performed over a period of years or decades. Different decay modes were investigated, including α, β^-, β^+ and EC decay. Residuals from the exponential nuclear decay curves were inspected for annual oscillations. The data sets were first compensated for (1) the presence of occasional outlier values, (2) abrupt systematic changes in the detector response, e.g. due to replacement of the electronics or recalibrations of the instrument, and (3) systematic drift extending over periods of more than 1 year.

This paper is part I of a trilogy, presenting experimental evidence for α decay. Part II [58] groups the evidence for beta minus decay and in part III [59] β^+ and EC decay are investigated. Graphs are shown of residuals of integrated count rates or ionisation currents (for convenience all types of signals will be represented by the same symbol, *I*) over the measured period, as well as multi-annual averages taken over fixed 8 d periods of the year. The uncertainty bars are indicative only: for the individual data they often refer to a short-range repeatability, and for the annual averaged data (maximum 46 data, covering 8 d periods) they were derived from the spread of the input data and the inverse square root of the number of values in each data group. As a reference measure for the expected solar influence, a functional curve is included representing the annual variation of the inverse square of the Sun–Earth distance, $1/R^2$, renormalized to an amplitude of 0.15% (which is the magnitude of the effect claimed by Jenkins *et al*). To the averaged residuals plotted as a function of time, a sinusoidal shape $A \sin(2\pi (t + a)/365)$ has been fitted in which A is the amplitude, t is the elapsed number of days since New Year, and a is the phase shift expressed in days. This function is occasionally included in the residual plots. A summary table of the sinus parameter fit values for each data set has been published in [60].

2. Radium-226 series

2.1. Decay characteristics

Radium-226 is typically used as a reference source for gamma-ray spectrometers and for ionisation chambers (IC) [61] acting as secondary standardisation devices for activity. The ^{226}Ra has a half-life of 1600 (7) a and decays by α-emission to ^{222}Rn

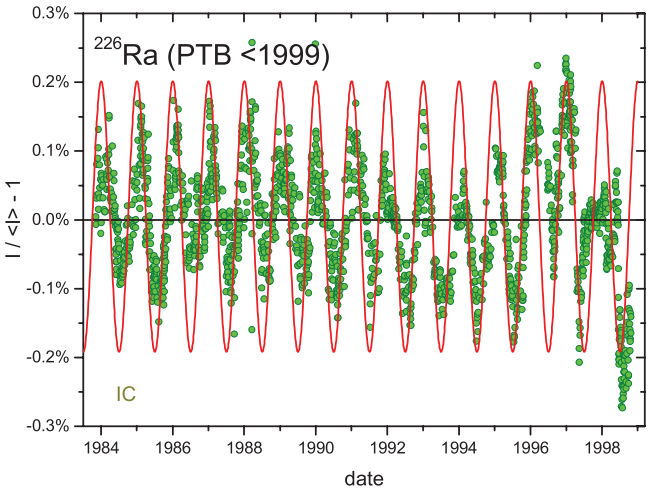

Figure 1. Residuals from an exponential decay curve of the ionisation current from a ^{226}Ra source inside the IG12/A20 ionisation chamber at PTB measured between 1984 and 1998. The line represents relative changes in the inverse square $1/R^2$ of the Earth–Sun distance, normalized to an amplitude of 0.2%.

(3.8232 (8) d), followed by a series of mostly short-lived alpha and beta emitters ($T_{1/2} < 5$ d), except for ^{210}Pb (22.23 (12) a) and ^{210}Po (138.3763 (17) d) [16]. To measure the activity of ^{226}Ra and its progeny in equilibrium, more than a century old material needs to be used in a closed configuration that is radon tight. After a sudden loss of ^{222}Rn, the activity of the first 2/3rd of the decay series would re-establish itself in a few weeks, whereas the last 1/3rd of the chain would remain in equilibrium with the activity of ^{210}Pb for decades. Only the half-lives of the α emitters ^{226}Ra and ^{210}Po and the β^- emitter ^{210}Pb are long enough to be relevant for explaining annual variations in the decay rates as a result of seasonal changes in the decay constants through solar influence.

2.2. ^{226}Ra series @PTB (<1999)

On several occasions, series of activity measurements obtained with an ionisation chamber (type IG12, 20th Century Electronics, UK) at the PTB [62–65] have been used by others [17, 22, 66–68] to make claims about a solar influence on decay constants. Metrologists of the PTB have always emphasized that variations in the ionisation current are caused by instrumental and environmental parameters in the laboratory [40, 42, 62–65]. Recent tests in the Khalifa university (Abu Dhabi, UAE) [69] have confirmed that activity measurements with several detector types are sensitive to environmental conditions, such as temperature, humidity and pressure. Nevertheless, Jenkins *et al* claimed that 'sensitivities to seasonal variations in the respective detectors are likely too small to produce the observed fluctuations' [18].

The most cited case is ^{226}Ra, used as reference source for IC stability checks. As shown in figure 1, the residuals from an exponential decay curve to old data obtained from 1983 to 1998 show annual periodicity of about 0.15% magnitude. These oscillation effects—also present in residuals for ^{85}Kr, ^{90}Sr, ^{108m}Ag, ^{133}Ba, and ^{152,154}Eu [58, 59]—have been

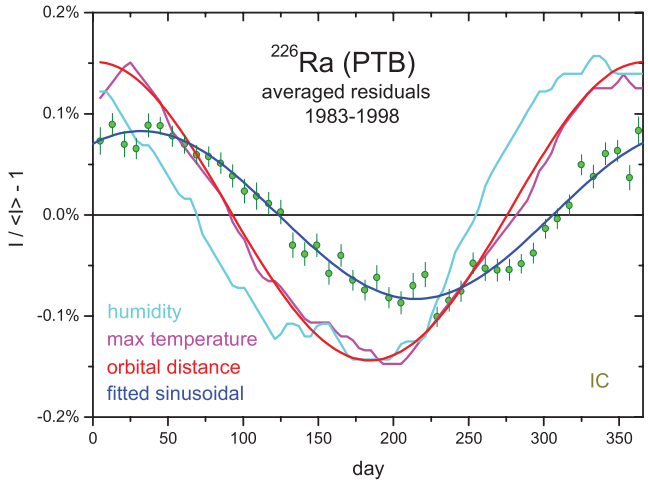

Figure 2. Annual averages of the residuals in figure 1 for periods of 8 d, compared to renormalised relative changes in $1/R^2$ for Earth–Sun distance as well as in the outdoor humidity and maximum temperature in the Braunschweig area. The sign of the temperature data was reversed to facilitate direct comparison.

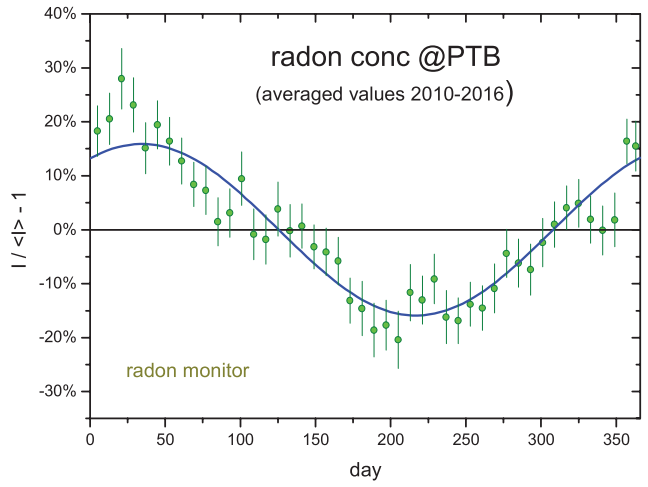

Figure 3. Annually averaged relative variations of radon concentration in the air inside the PTB laboratory room where the IC is installed, measured with a radon monitor from mid 2010 up to mid 2016. The line represents a sinusoidal function fitted to the data. The annual oscillations in radon concentration appear to be in phase with the modulations of the ^{226}Ra ionisation current in figure 2.

significantly reduced when the Townsend balance current measurement method was replaced by a commercial Keithley electrometer [42, 65] (see next section). Consequently, the effect is of instrumental nature and should not be interpreted as an indication of changing decay constants.

Figure 2 shows the averaged residuals grouped in bins of 8 d in the year, which take a sinusoidal shape as a function of time in which the amplitude is $A = 0.083$ (2) % and the phase shift $a = 59$ d. The phase does not coincide with the variations of orbital distance Earth–Sun ($a = 89.5$ d), nor with average humidity and temperature in the Braunschweig region [70]. Semkow *et al* [71] proposed an explanation through ambient conditions in the laboratory, however some of their arguments were criticised by Schrader [65]. The discharge of the capacitor through radon decays in the air, as suggested by Siegert *et al* [62], is a possible explanation, considering that the seasonal

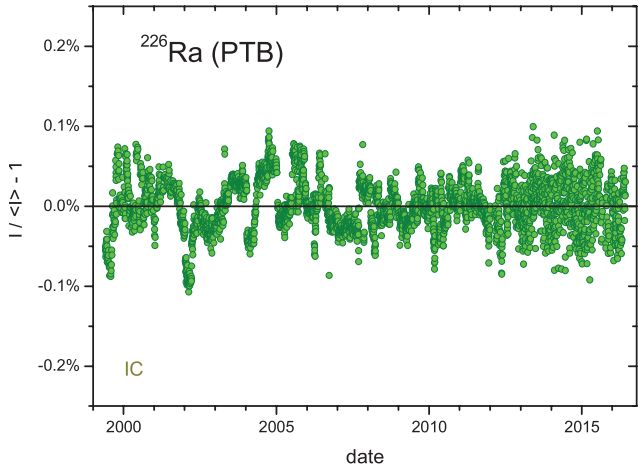

Figure 4. Residuals from exponential decay for ^{226}Ra ionisation current measurements with the PTB IG12/A20 ionisation chamber from 1999 to 2016.

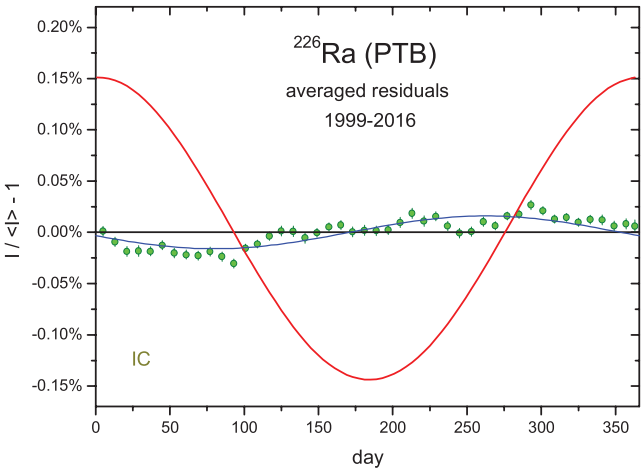

Figure 5. Annual average residuals from exponential decay for ^{226}Ra ionisation current measurements with the PTB IC from 1999 to 2016. The modulations are smaller than in figure 2 due to a replacement of electronics.

variations for atmospheric radon concentration follow a sinusoidal model [72]. There is indeed a remarkable correlation with average seasonal changes of radon concentration in air ($A = 16$ (2)%, $a = 57$ d) measured inside the laboratory from 2010 to 2016 (see figure 3), but causality has not been proved.

2.3. *^{226}Ra series @PTB (>1999)*

The ^{226}Ra data collected with the same IC from 1999 to 2016 are presented in figure 4. Since the replacement of the Townsend balance with commercial electrometers Keithley 6517A and B [42, 65], the annual modulations have reduced drastically and their phase has changed as well. The annually averaged residuals in figure 5 now show a modulation with an amplitude of $A = 0.016$ (1)% and a phase shift of $a = 194$ d. This measurement series shows mild correlation with the room temperature (figure 6, $\rho = 0.23$) and humidity (figure 7, $\rho = 0.25$), but not with the radon concentration in the laboratory (figure 3, $\rho = 0.0$). Nähle and Kossert [42] already pointed out that temperature and humidity can have an effect on the electrical

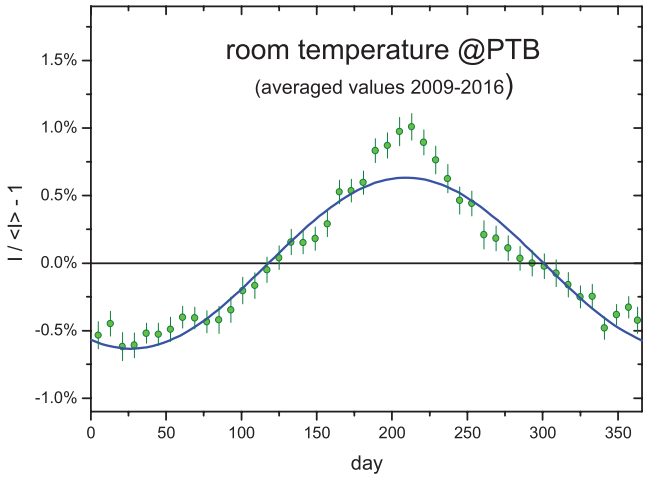

Figure 6. Annually averaged relative variations of the room temperature (in kelvin) inside the PTB laboratory from 2009 to 2016.

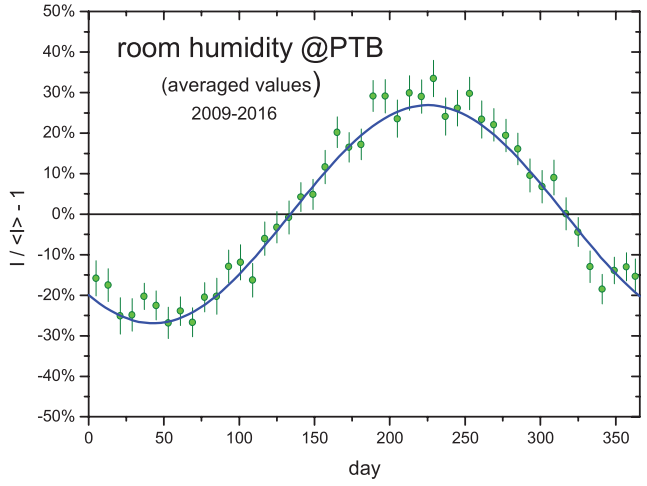

Figure 7. Annually averaged relative variations of the relative humidity inside the PTB laboratory from 2009 to 2016.

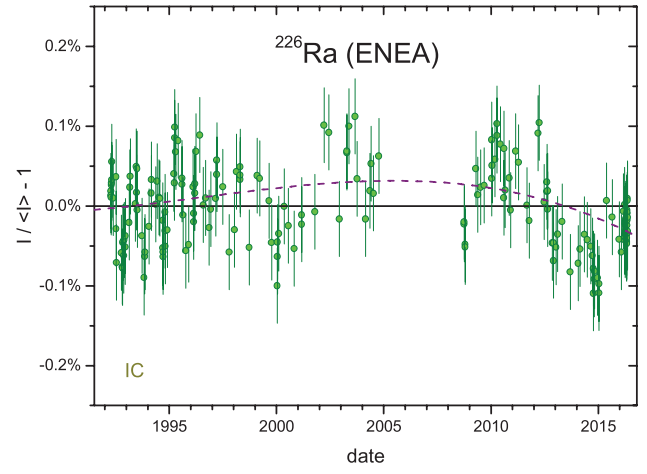

Figure 8. Residuals from exponential decay for ^{226}Ra ionisation current measurements with the IG11 IC at ENEA between 1992 and 2016. The dashed line shows a trend line fitted to the data.

properties of the signal cables and the electrometer. The manufacturer of the Keithley electrometers used at PTB claims a

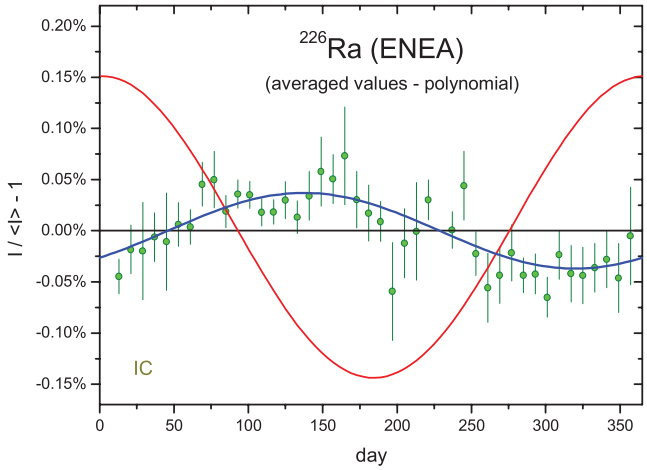

Figure 9. Annual average residuals from exponential decay for ^{226}Ra activity measurements with the ENEA IC, in which the input data were first detrended by means of the trend line in figure 8.

temperature coefficient of 0.1%/°C of the reading in the relevant current range (see [42] and references therein).

2.4. *^{226}Ra series @ENEA*

At ENEA (Italy) between 1992 and 2016, 213 ionisation current measurements were performed on a ^{226}Ra source, using a Centronic IG11 ionisation chamber with a Keithley 617 electrometer. The decay-corrected current measurements cover a period of 24 years and have a standard deviation of 0.05%. The residuals from exponential decay are presented in figure 8, together with a polynomial trend line fitted to the data. By compensating for this sub-permille trend line, the standard deviation of the residuals could be reduced to 0.04%. Whereas annual sinusoidal oscillations are not immediately apparent from the individual residuals, they do appear in the annual average (detrended) residuals in figure 9 with an amplitude of $A = 0.037\ (4)\%$ and a phase of $a = 319$ d. Without the detrending correction, the modulation of the data is less smooth and the fitted amplitude is lower ($A = 0.026\ (6)\%$, $a = 305$ d). The modulations are not in phase with Earth–Sun distance, nor with the PTB data, therefore are unlikely to be generated by the same global phenomenon.

Between 24 March and 12 May 2016, thousands of systematic measurements have been performed to investigate correlations between the IC readouts for a ^{226}Ra source and room temperature, ambient pressure, relative humidity and radon concentration in air in the same laboratory room. The graphs in figure 10 illustrate the significant correlation ($\rho = 0.84$) between temperature and (averaged) IC currents, whereas the other environmental conditions have a lower impact ($-0.2 < \rho < 0.2$). This suggests that the seasonal variations in the IC signals at ENEA may find their origin in temperature variations in the laboratory.

Since multiple measurements were performed during day and night, the readouts could be investigated for diurnal modulations as well. For each hour of the day an average value was calculated. The average temperature over this 49 d period

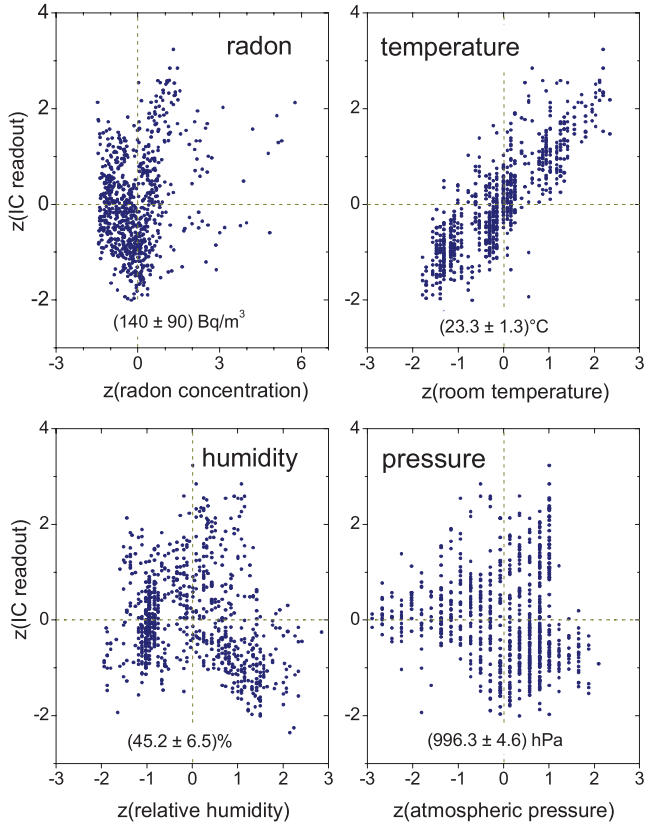

Figure 10. Correlation plot of averaged ^{226}Ra current readouts in the ENEA IC with radon concentration in air, room temperature, relative humidity and atmospheric pressure measured from March to May 2016 in the ENEA laboratory. The data were rescaled to a z-score using $z = (x - \mu)/\sigma$.

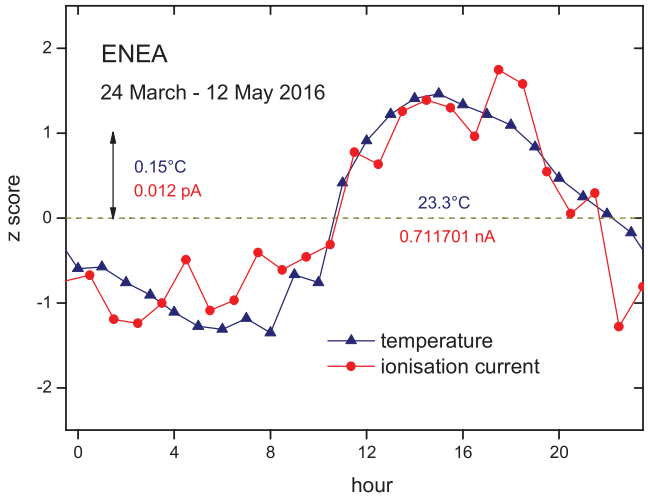

Figure 11. Z-score plot of diurnal variations in the ^{226}Ra current and room temperature at the ENEA laboratory, averaging readouts collected between 24 March and 12 May 2016.

shows a daily cycle with minimum values (23.08 °C) in the morning and maximum values (23.50 °C) in the afternoon. The average IC current shows nominally less variation (0.005%), but follows a similar pattern. The close correlation between the IC current and temperature variations are immediately apparent when plotting them as a z-score ($z = (x - \mu)/\sigma$) as a function of time, as shown in figure 11. Since the diurnal

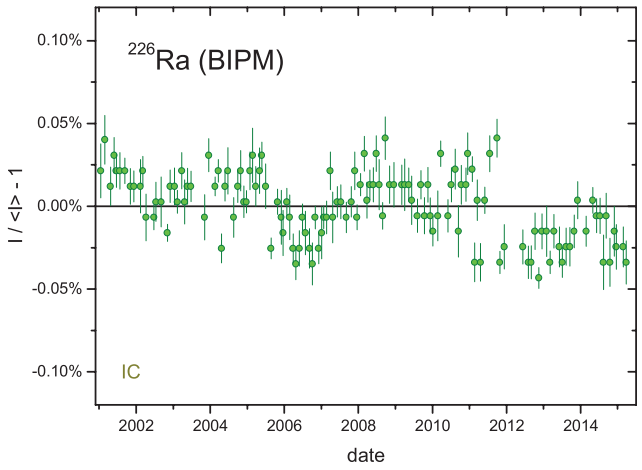

Figure 12. Residuals from exponential decay for ^{226}Ra activity measurements with an IG11 ionisation chamber of the SIR at the BIPM.

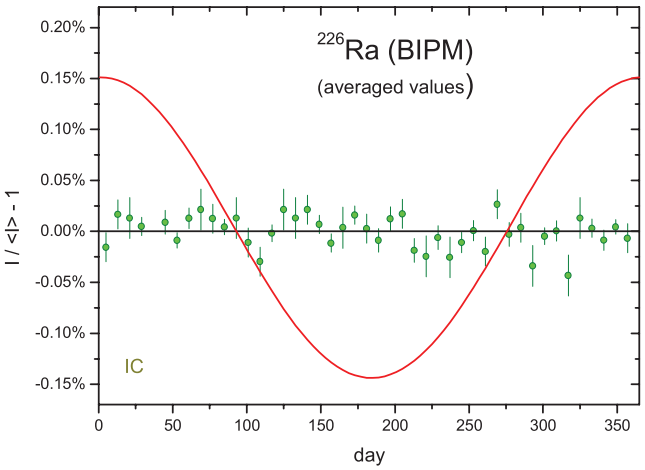

Figure 13. Annual average residuals from exponential decay for ^{226}Ra activity measurements with the BIPM IC.

modulations in the IC are proportional to and synchronous with the temperature changes, causality may be inferred. The specifications of the electrometer mention a temperature coefficient of 0.15%/ °C in the 200 pA range. The correlation plots reveal a slope of 0.1%/°C for an average current of 0.71 nA. This study is a good illustration of the point raised that one should rule out instrumental uncertainties before reverting to new physics [2, 36, 37].

2.5. *^{226}Ra series @BIPM*

The BIPM (located in France) houses the SIR [33], a system of two Centronics IG11 ICs used as long-term reference instruments by which mono-radionuclide solutions with standardised activities can be compared for equivalence. The stability of the SIR is monitored with ^{226}Ra check sources and the residuals from exponential decay between 2001 and 2015 for source #4 in IC #389 are presented in figure 12. The residuals are small, mostly within 0.05%, and in the annual averages of figure 13 the residual sinusoidal effect—if any—appears to be in the order of $A = 0.004$ (3)% and phase $a = 4$ d. This is an order of

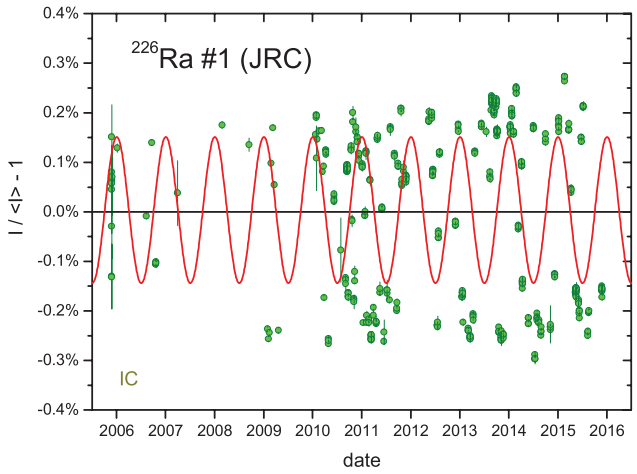

Figure 14. Residuals from exponential decay for ^{226}Ra (source #1) activity measurements with the IG12 IC of the JRC.

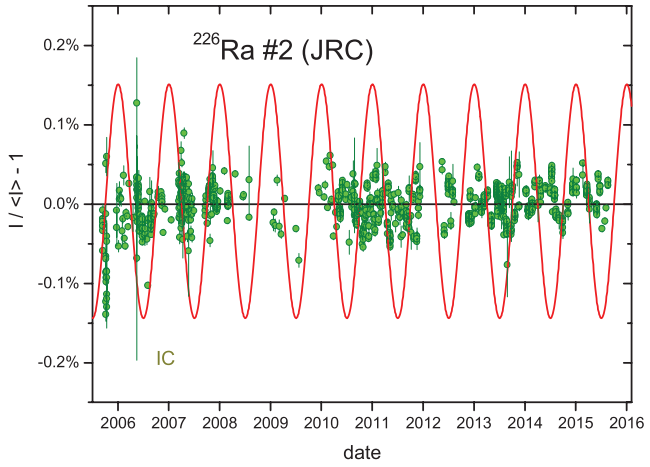

Figure 15. Residuals from exponential decay for ^{226}Ra (source #2) activity measurements with the IG12 IC of the JRC.

magnitude smaller than the natural dispersion of the data, out of phase with Earth–Sun distance, and firm evidence of the invariability of the ^{226}Ra decay constant to solar proximity.

2.6. ^{226}Ra series @JRC

The Joint Research Centre (JRC) of the European Commission contributes to the establishment of a common measurement system of activity through its radionuclide metrology laboratory in Geel (Belgium). Two ^{226}Ra sources (#1 and #2) are frequently measured in the IG12 well-type IC (20$^{\text{th}}$ Century Electronics, UK) filled with argon to 2 MPa. The ionisation current is measured by sampling a voltage over an external feedback air-spaced capacitor [73]. In off-line data analysis, it is corrected for average background signal and decay.

Figures 14 and 15 show the residuals from a smooth decay curve obtained between 2005 and 2015 with sources #1 and #2, respectively. The current readouts (66 pA) from source #1 reveal a bimodal pattern, tentatively ascribed to occasional leakage of radon and progeny from the metal container. Source

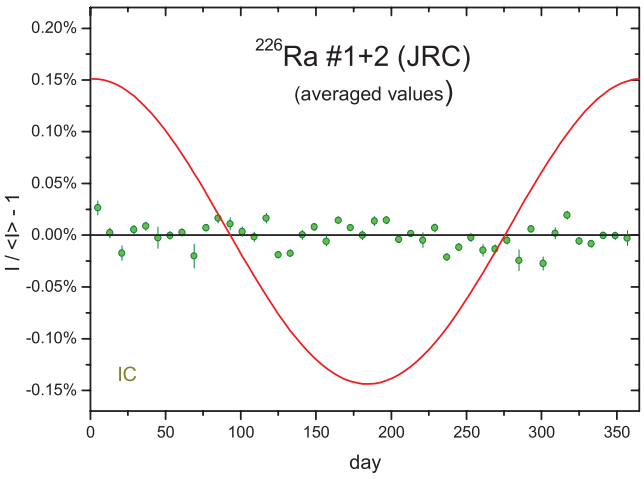

Figure 16. Annual average residuals from exponential decay for ^{226}Ra activity measurements with the IG12 IC of the JRC, taken as a weighted mean for sources #1 and #2.

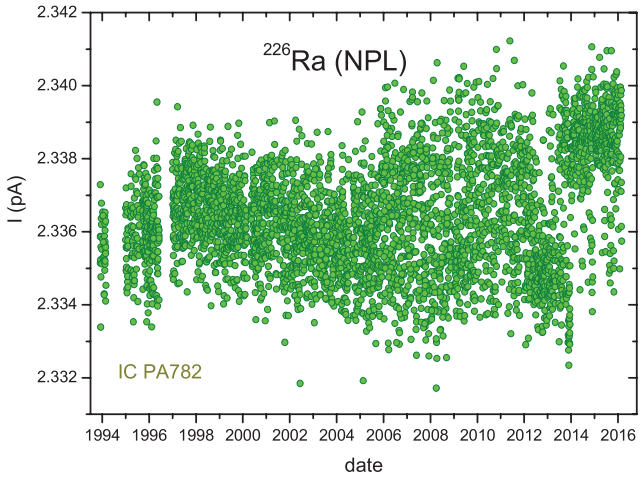

Figure 17. Decay-corrected ionisation current of a ^{226}Ra source with the PA782 IC of NPL, in which different calibration factors were applied over periods in time.

#2 is more active and its residuals are much smoother, however its decay-corrected current (139 pA) had to be compensated for a quasi-parabolic increase of 0.092% in 10 years. The latter is likely due to ingrowth of ^{210}Pb, assuming that the ^{226}Ra was not in perfect equilibrium with its daughter nuclides when the source was produced. A weighted mean of the weekly averages of the residuals is presented in figure 16: there is no indication of an annual effect ($A = 0.003\ (2)\%$, $a = 363$ d).

2.7. ^{226}Ra series @NPL

At the NPL (UK) ICs are intensively used for secondary standardisation of activity. A long history of ^{226}Ra check source measurements were provided for two well-type re-entrant ICs: a PA782 (2 MPa argon gas, steel inner well) and a Vinten (1 MPa nitrogen gas, 3 mm Al inner well). Figure 17 shows 4306 raw decay-corrected current readouts in the PA782 from 1993 to 2016. The apparent small systematic shifts are caused by application of changing calibration factors. The data were analysed in a pragmatic manner by applying a renormalisation for every

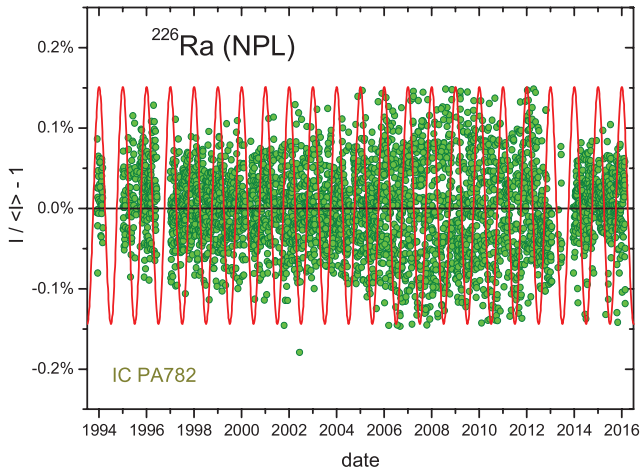

Figure 18. Residuals from exponential decay for ^{226}Ra activity measurements with the PA782 IC of NPL, after normalisation per calendar year.

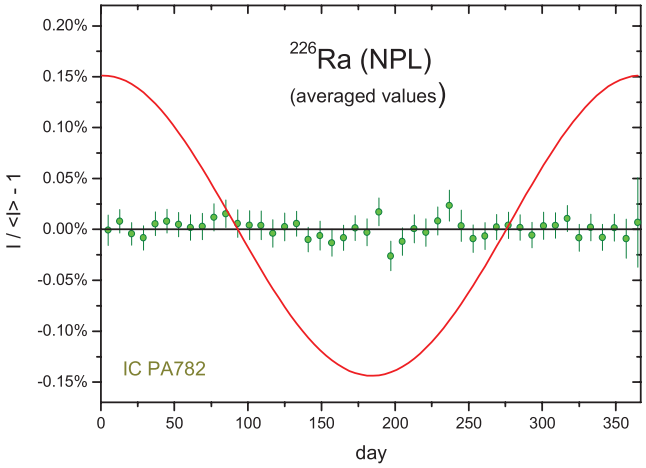

Figure 19. Annual average residuals from exponential decay for the renormalized ^{226}Ra activity measurements with the PA782 IC of NPL.

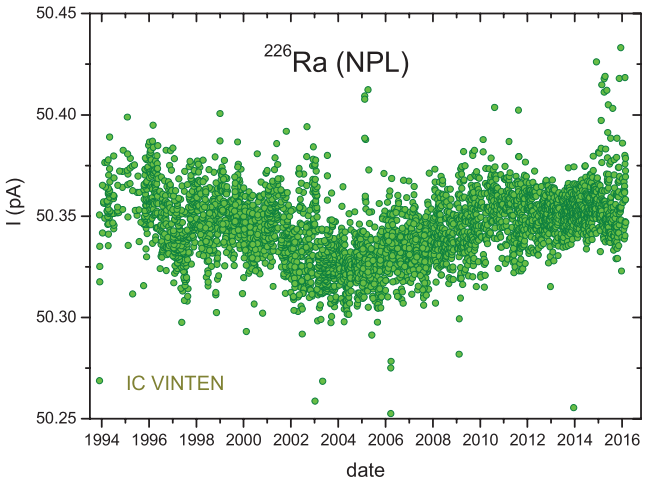

Figure 20. Decay-corrected ionisation current of a ^{226}Ra source with the Vinten IC of the NPL, in which different calibration factors were applied over periods in time.

calendar year and elimination of 6% data at both extremes, resulting in the individual residuals of figure 18 and the averages

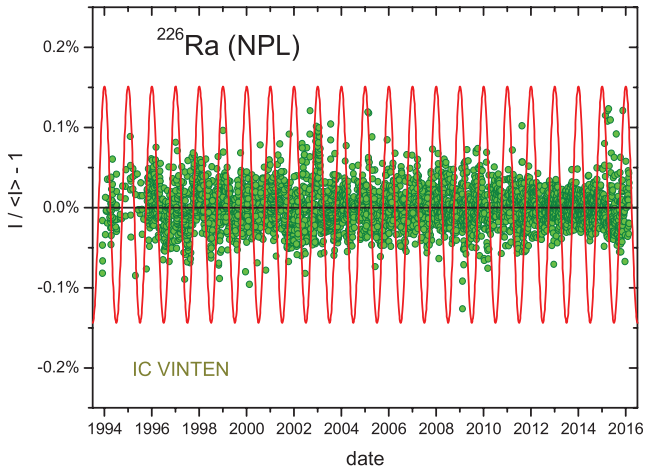

Figure 21. Residuals from exponential decay for ^{226}Ra activity measurements with the Vinten IC of NPL, after renormalisation per calendar year.

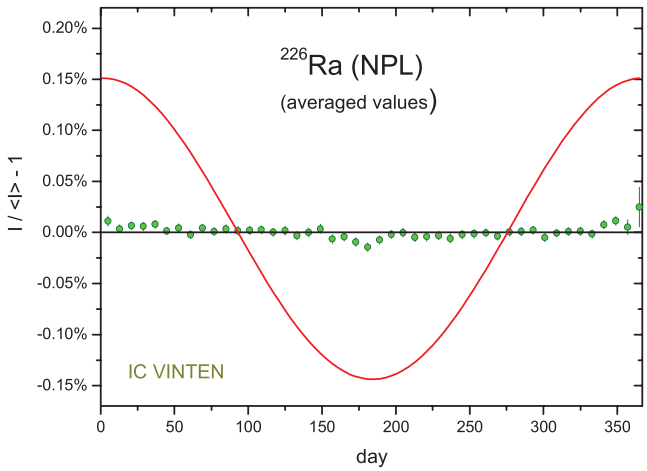

Figure 22. Annual average residuals from exponential decay for the renormalized ^{226}Ra activity measurements with the Vinten IC of NPL.

in figure 19. These data represent conclusive evidence that there is no annual effect ($A = 0.0025\ (18)\%$, $a = 60$ d).

The 4017 current readouts obtained with the Vinten (figure 20) show even less dispersion, but make noticeable jumps on long-term due to recalibrations. Applying renormalisation per calendar year and removal of 0.6% of extreme data, the residual plot in figure 21 was obtained and the averages in figure 22. In spite of the crude renormalisation procedure, there is only a small residual trend in the annual averages ($A = 0.005\ (1)\%$, $a = 73$ d).

2.8. ^{226}Ra series @NMISA

Additional evidence was collected from the southern hemisphere, at NMISA (South Africa) and ANSTO (Australia) (see next section). The ^{226}Ra readouts between 1994 and 2015 (figure 23) in the Isocal IV well-type IC at NMISA showed large variability and regular adjustments were done to keep them within specifications. The averages in figure 24 do not have the required precision to make statements about

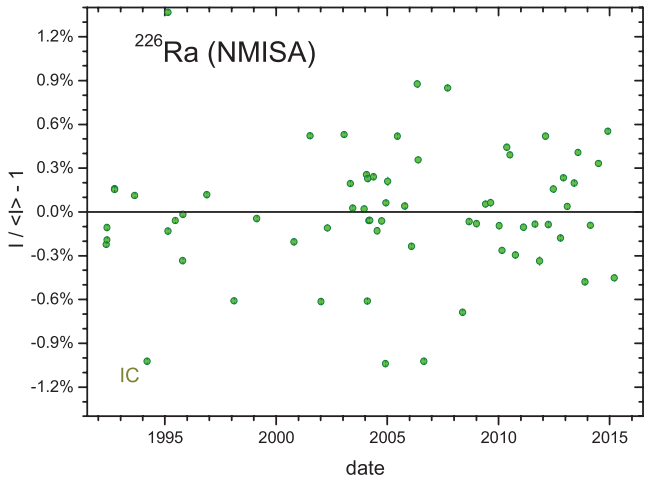

Figure 23. Residuals from exponential decay for ^{226}Ra activity measurements with the IC of NMISA.

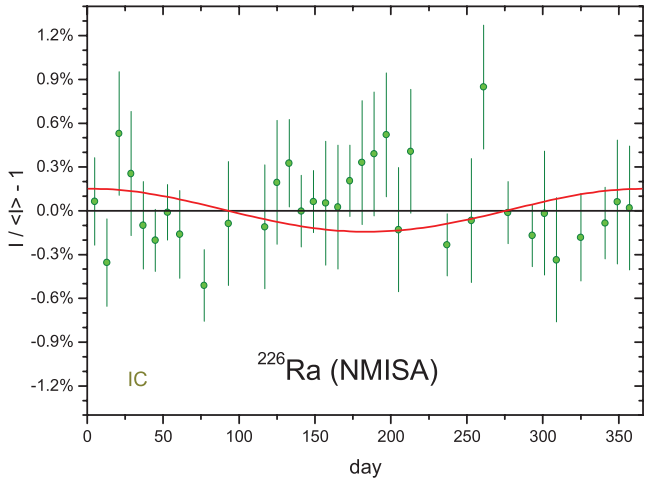

Figure 24. Annual average residuals from exponential decay for the ^{226}Ra activity measurements with the IC of NMISA.

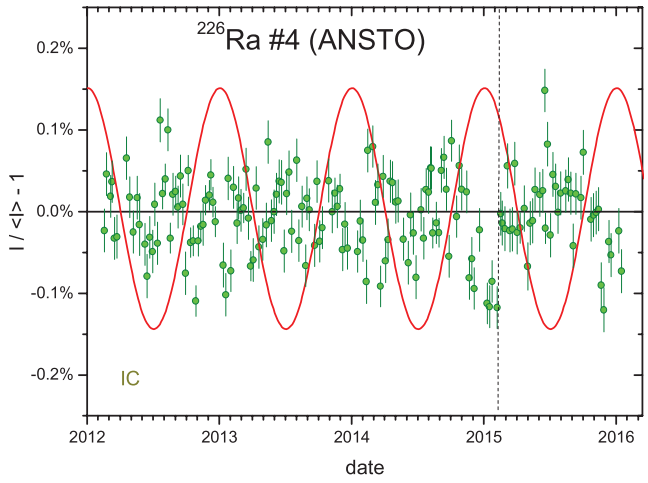

Figure 25. Residuals from exponential decay for ^{226}Ra (source #4) activity measurements with the TPA Mk-II IC of ANSTO.

sub-permille variations, but this case exemplifies the notion that instrumental instabilities can be significant and should be considered prior to postulating new physics.

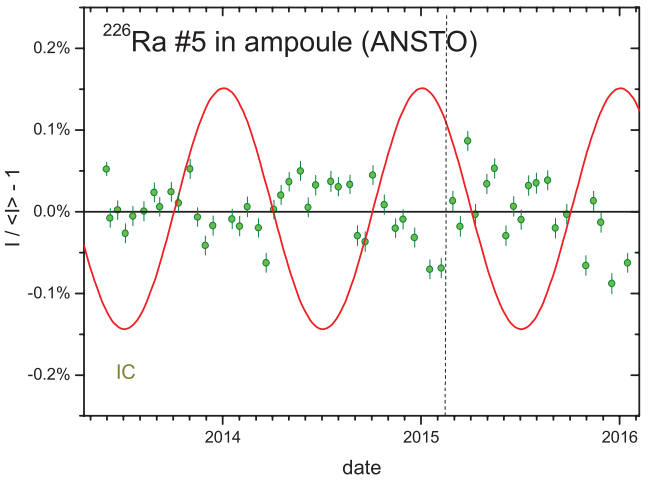

Figure 26. Residuals from exponential decay for ^{226}Ra (source #5 in an ampoule) activity measurements with the IC of ANSTO. The dotted line marks the installation of a new electrometer.

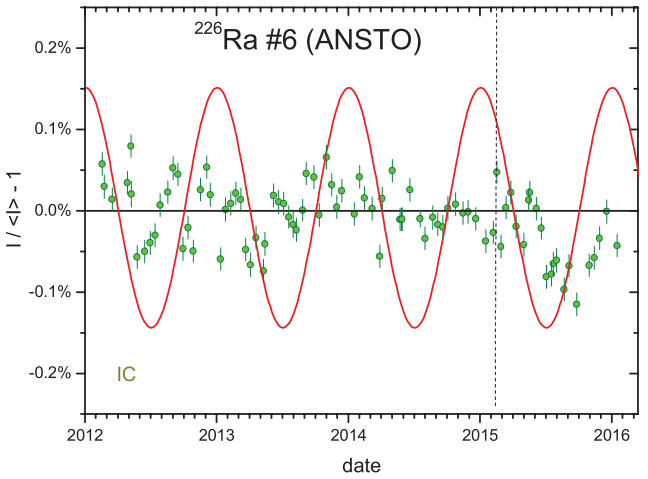

Figure 27. Residuals from exponential decay for ^{226}Ra (source #6) activity measurements with the IC of ANSTO. The dotted line marks the installation of a new electrometer.

2.9. ^{226}Ra series @ANSTO

ANSTO (Australia) provided 9 data sets of IC measurements of ^{226}Ra sources#1, #3, #4, #5, #6, #7 in standard as well as special configurations (source #4 in vial, #5 in ampoule, and #7 in Al Au). The IC is a TPA Mk-II filled with 2 MPa of argon and operated at a bias of 520 V. Ionisation current is measured with a Keithley 6517A electrometer. A selection of 4 sets of residuals from an exponential curve are presented in figures 25–28. All data were renormalised after mid February 2015, when a new electrometer was brought in use. The latter had a noticeable effect on the background current and readout for low-activity sources. In figure 29 a mean is shown from 7 data sets for sources #4–7. There is some residual time dependence, but annual effects are negligibly low ($A = 0.005$ (3)%, $a = 256$ d) also in the southern hemisphere.

ANSTO kept additional records of the response of a medical calibrator (TPA ionisation chamber with Keithley electrometer) to a ^{226}Ra reference source. The statistical precision of these data is in the 1% range (see figure 30), but averages of the 1749

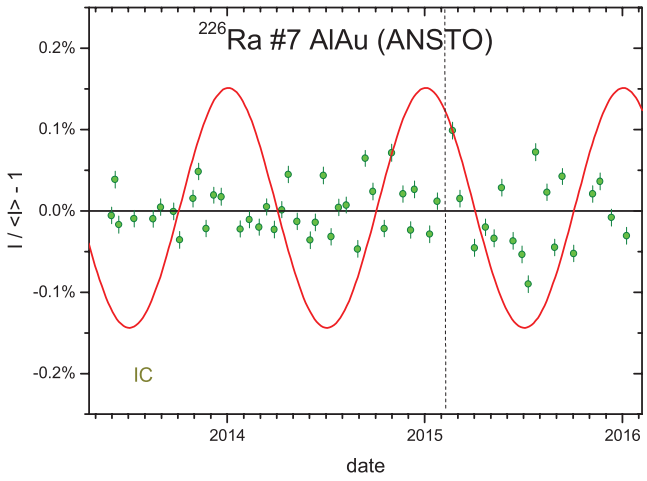

Figure 28. Residuals from exponential decay for ^{226}Ra (source #7 in Al–Au) activity measurements with the IC of ANSTO. The dotted line marks the installation of a new electrometer.

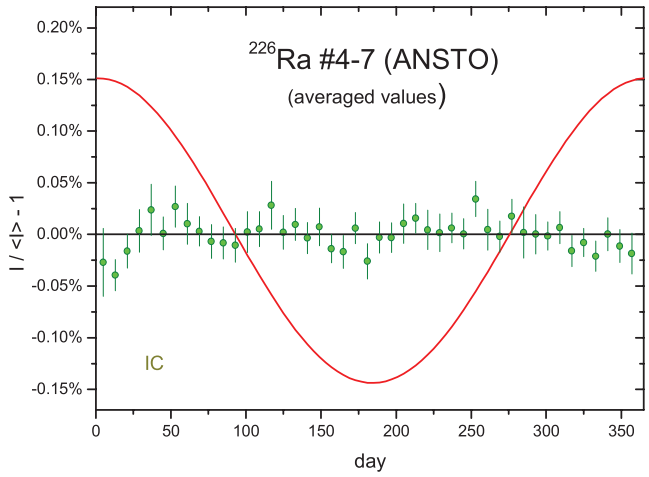

Figure 29. Annual average residuals from exponential decay for ^{226}Ra (7 data sets for sources #4–7) activity measurements with the IC of ANSTO.

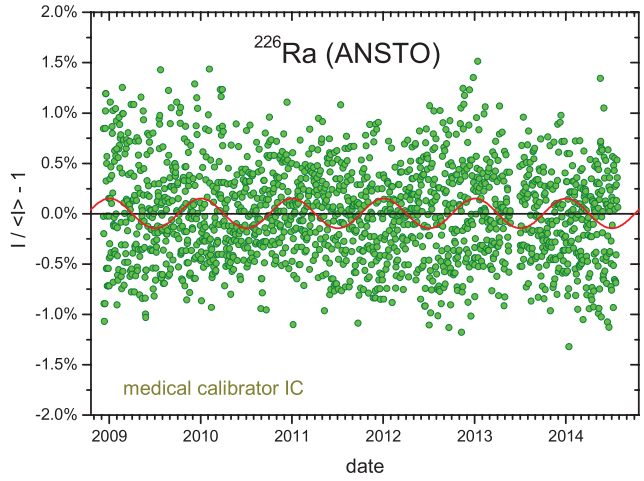

Figure 30. Residuals from exponential decay for ^{226}Ra activity measurements with a medical calibrator (IC) of ANSTO.

data points obtained between 2009 and 2015 demonstrate the absence of annual oscillations at the10^{-3} level (figure 31).

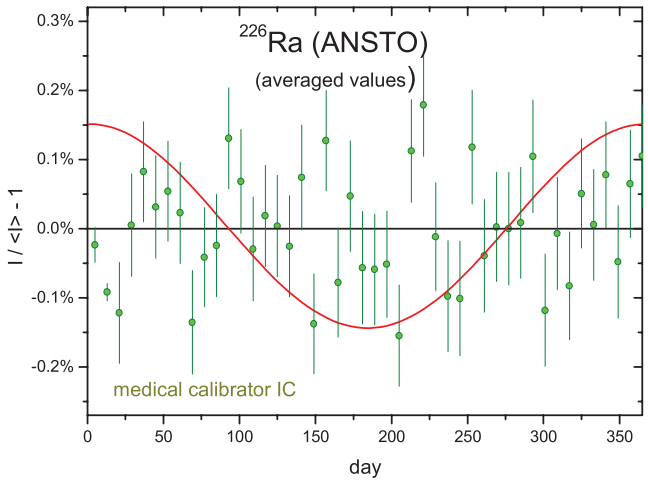

Figure 31. Annual average residuals from exponential decay for ^{226}Ra activity measurements with a medical calibrator (IC) of ANSTO.

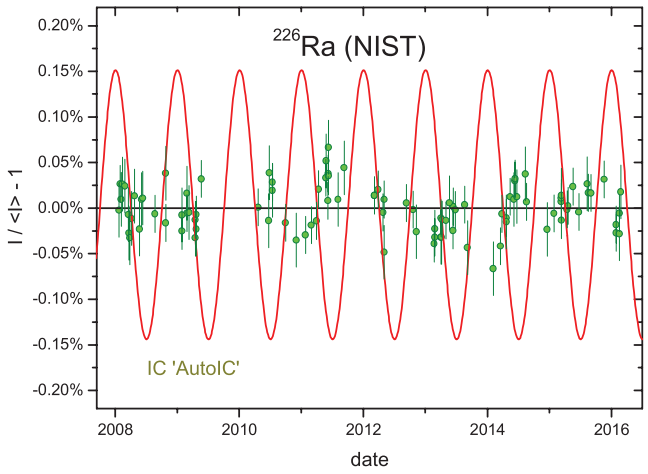

Figure 32. Residuals from exponential decay for activity measurements of two ^{226}Ra sources with the 'AutoIC' of NIST.

2.10. ^{226}Ra series @NIST

At the NIST, two ^{226}Ra sources were measured in total 99 times in the 'AutoIC' ionisation chamber [74] between 2008 and 2016 (figure 32). The AutoIC consists of a Centronic IG11 re-entrant IC shielded by lead on all sides. The detector bias is negative 1.10 kV and the ionisation current is measured by a Keithley 6517A digital electrometer (Keithley Instruments, Inc, Cleveland, OH, USA). The samples are loaded into the chamber by a custom-designed automatic sample changer. Instrument stability is regularly checked with sealed ^{226}Ra needle sources encapsulated in acrylic right-circular cylinders. The mean residuals in figure 33 show a mild annual modulation ($A = 0.015\ (3)\%$, $a = 255$ d).

An additional set of 272 ^{226}Ra measurements were performed between 2012 and 2016 in the NIST Vinten 671 IC ('VIC') [75] (serial number 3–2, Vinten Instruments, Surrey, UK), which is biased to 1500 V and is also read by a Keithley 6517A electrometer. The data of the VIC have a larger variance compared to the AutoIC (figure 34),

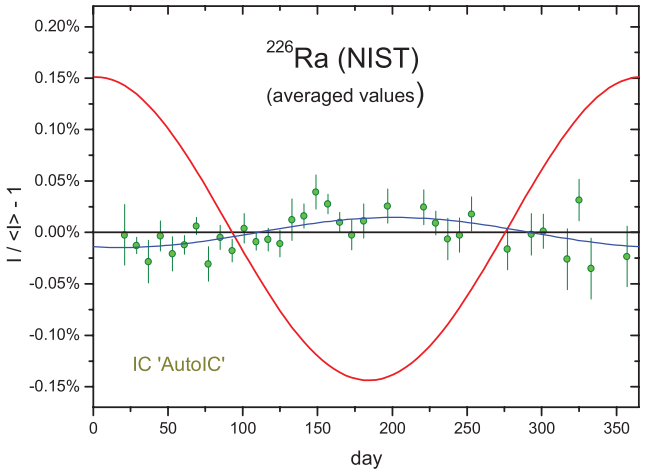

Figure 33. Annual average residuals from exponential decay for ^{226}Ra activity measurements with the 'AutoIC' of NIST.

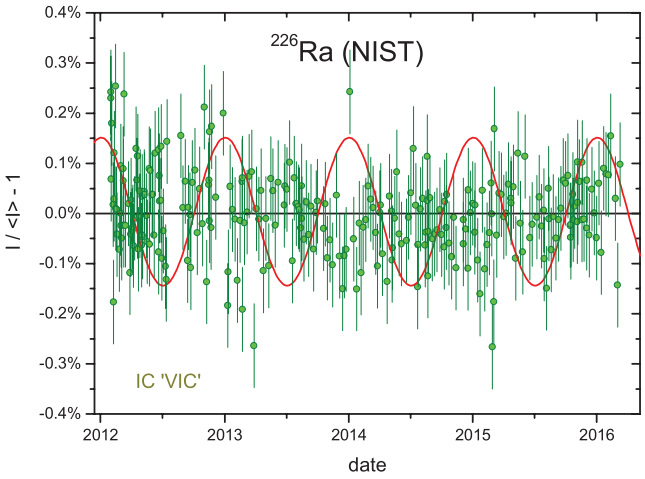

Figure 34. Residuals from exponential decay for ^{226}Ra activity measurements with the 'VIC' of NIST.

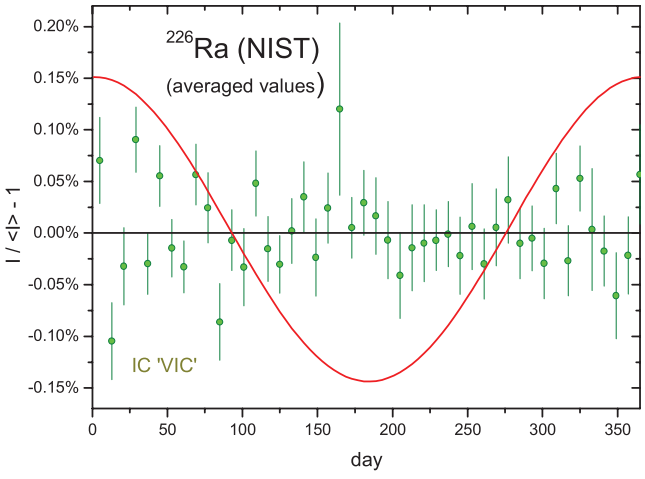

Figure 35. Annual average residuals from exponential decay for ^{226}Ra activity measurements with the 'VIC' of NIST.

but the average residuals (figure 35) show no annual trend ($A = 0.002$ (8)%, $a = 8$ d). The modulations in the AutoIC data are therefore not driven by a common effect on the decay constants.

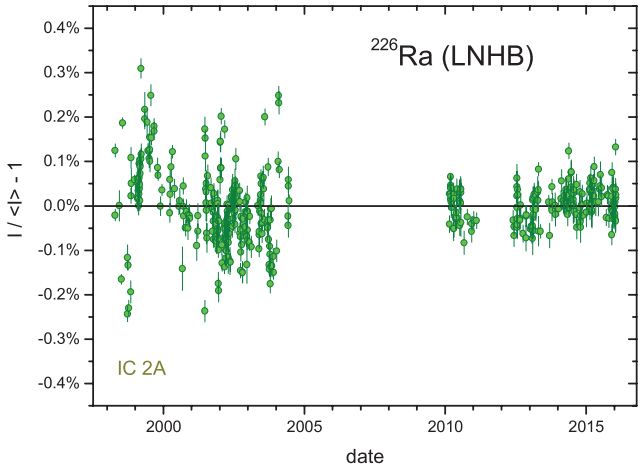

Figure 36. Residuals from exponential decay for ^{226}Ra activity measurements with the IC 2A of LNHB.

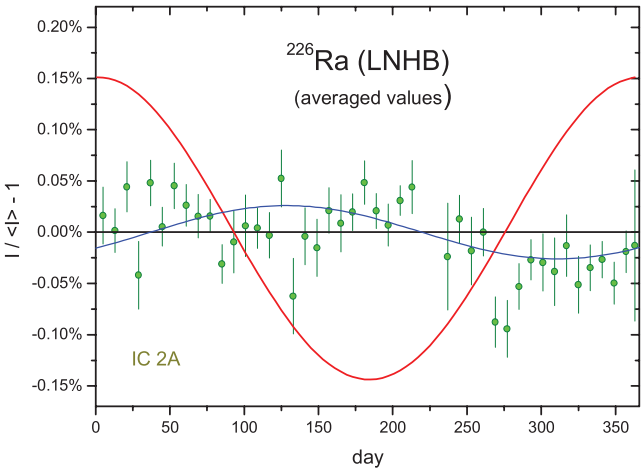

Figure 37. Annual average residuals from exponential decay for ^{226}Ra activity measurements with the IC 2A of LNHB.

2.11. ^{226}Ra series @LNHB

At the LNHB (France), ^{226}Ra measurements were performed between 1998 and 2016 in ICs 2A and 6D. The IC 2A is a 1 MPa nitrogen-filled Vinten 671 (Centronic, UK) and the IC 6D is a Vacutec 70129 (Nuklear-Medizintechnik Dresden GmbH, Germany) filled with a 1.1 MPa mixture of xenon and argon gas. Both ICs have an aluminium alloy wall, are surrounded by a 5-cm-thick lead shield, and their current is read out with a Keithley 6517A electrometer. The −400 V high voltage of both ICs is supplied by the electrometer. The ^{226}Ra ionisation current data obtained with the IC 2A were linearised, a few outliers removed, and the 455 residuals are presented in figure 36. The mean residuals in figure 37 show a mild annual modulation of $A = 0.026$ (6) % and $a = 328$ d. The same data treatment was performed on the IC 6D, resulting in the 499 residuals in figure 38. The amplitude of the annual modulations (figure 39) in this device is twice as high as in the IC 2A and the phase is slightly different: $A = 0.042$ (7) % and $a = 294$ d.

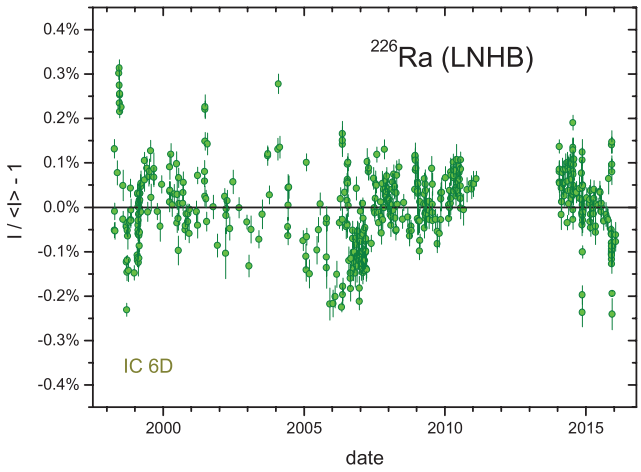

Figure 38. Residuals from exponential decay for ^{226}Ra activity measurements with the IC 6D of LNHB.

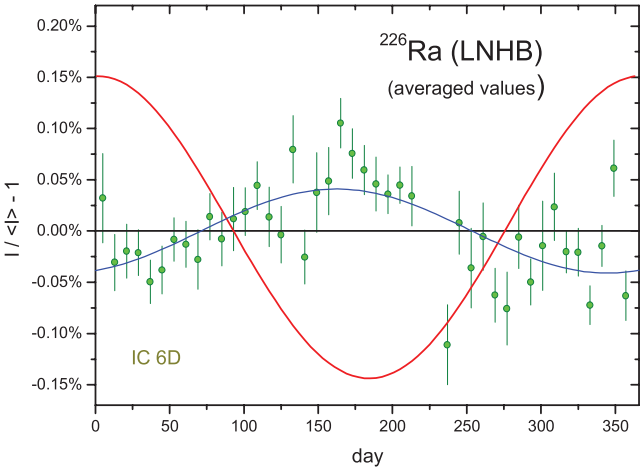

Figure 39. Annual average residuals from exponential decay for ^{226}Ra activity measurements with the IC 6D of LNHB.

3. Polonium-209

3.1. Decay characteristics

Polonium-209 (122.9 (23) a) decays by α emissions (99.546 (7)%) to excited levels and the ground state level of ^{205}Pb and by EC (0.454 (7)%) to the 896 keV excited level of ^{209}Bi.

3.2. ^{209}Po @JRC

Pommé and Benedik [76] published an improved half-life value for ^{209}Po based on the continuous measurement of emitted alpha particles from two drop-deposited sources in close geometry with a planar silicon detector (PIPS©). The decay curve of source #1 is presented in figure 40 (and of source #2 in [76]). The residuals are purely of statistical nature, and therefore the annual oscillations in figure 41 ($A = 0.006$ (5)%, $a = 6$ d) are insignificant. This type of measurement is quasi-free of interference because the alpha particles have a high energy of 5 MeV and can be easily

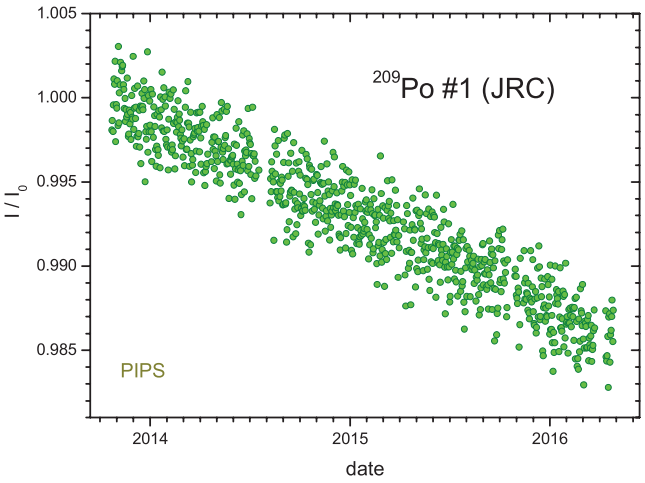

Figure 40. Measured relative alpha-particle count rates from the decay of ^{209}Po source #1 with a planar silicon detector at JRC, not corrected for decay.

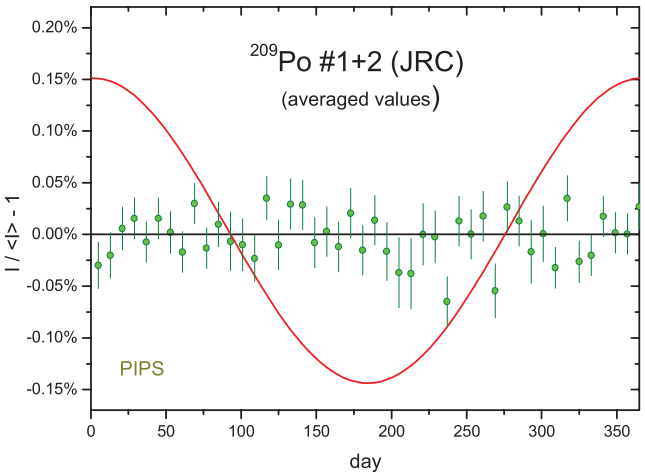

Figure 41. Annual average residuals from exponential decay for ^{209}Po activity measurements with a planar silicon detector at JRC.

separated from electronic noise in the detection chain. The background signal is close to zero and the geometry was stable because the ^{209}Po source was resting in a source mount placed directly on the detector housing in a vacuum chamber and the whole set-up remained untouched for two years.

4. Americium-241

4.1. Decay characteristics

Americium-241 (432.6 (2) a) decays 100% by α emission to ^{237}Np, mostly populating the excited level at 59.54 keV. There is a small spontaneous fission branch of 3.6 (9) $\times$ 10^{-10} %. Two (partly converted) characteristic γ transitions useful for spectrometer calibration at low energy are 26.34 keV and 59.54 keV. The main alpha emission energy is at 5.5 MeV. This radionuclide is frequently used in calibration sources for gamma and alpha spectrometry.

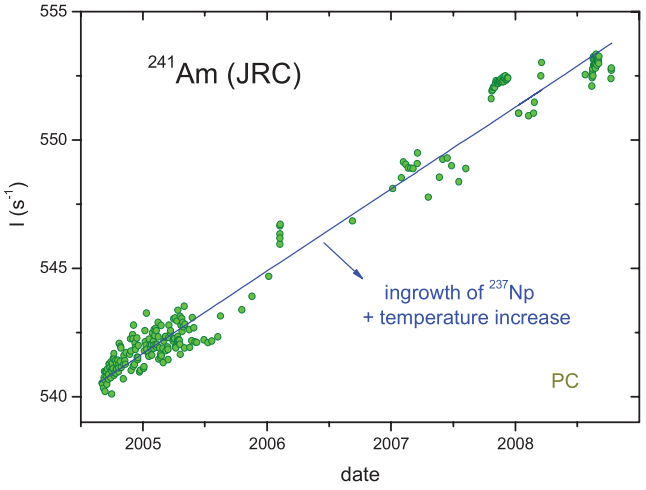

Figure 42. Measured count rate from photon (and electron) emission in the decay of ^{241}Am with a gas-filled proportional counter in fixed low solid angle geometry at JRC.

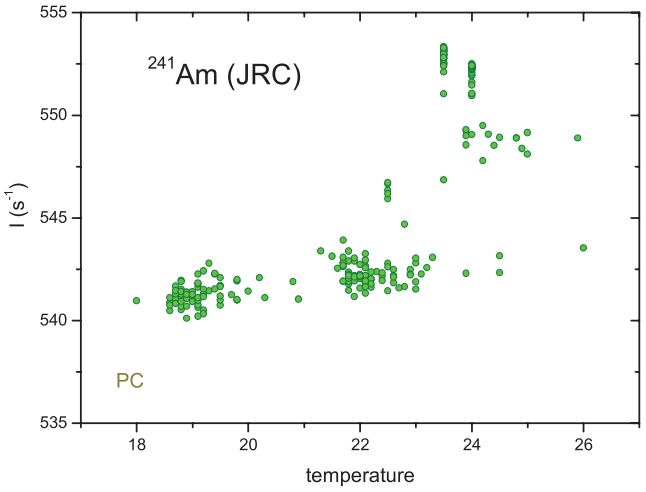

Figure 43. Measured count rate from the decay of ^{241}Am with a proportional counter as a function of temperature in the laboratory at JRC.

4.2. *^{241}Am @JRC*

Whereas the ^{209}Po experiment in section 2.8 is an example of how an alpha emitter can be measured free of interference and with stable counting efficiency, the opposite can be realised by applying unfavourable measurement conditions. At the JRC, an ^{241}Am source was used for checking the stability of an x-ray counter with defined solid angle [77] in the frame of an ^{55}Fe half-life experiment [78] (see part II [58] of this trilogy), but eventually turned out to be unsuited for the task. The alpha particles were stopped by a Be window and the photons were measured in a proportional counter (PC) at a counter gas pressure of 1.14×10^5 Pa (compared to a reference pressure vessel). The count rate (figure 42) appeared to increase as a function of time, tentatively ascribed to the ingrowth of ^{237}Np and/or rising of the room temperature from 19 °C to 22 °C and later 24 °C (figure 43). Possibly, small changes in the detector volume and threshold settings may have affected the counting efficiency for the wide range of photons (and conversion

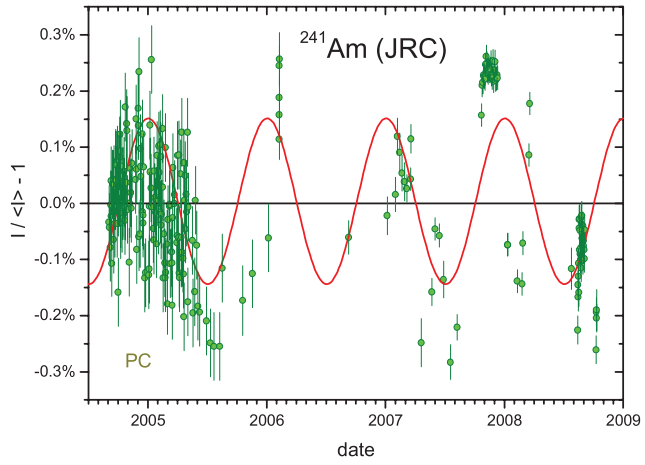

Figure 44. Residuals from exponential decay for ^{241}Am activity measurements with a proportional counter at JRC.

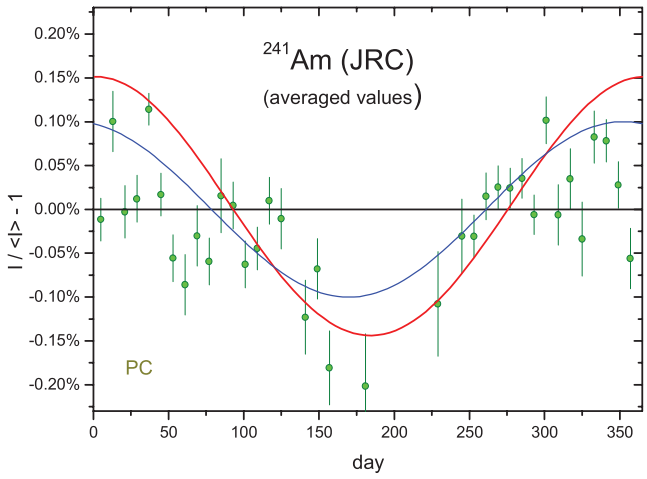

Figure 45. Annual average residuals from exponential decay for ^{241}Am activity measurements with a proportional counter at JRC (comprising all data from figure 44).

electrons) emitted in ^{241}Am and ^{237}Np decay (figure 44), whereas for the 0.6–6 keV x-rays from ^{55}Fe it remained fairly stable (close to 100% efficiency). The instabilities in the measurement conditions seemingly support the idea of variability of decay constants (figure 45) with an amplitude of $A = 0.101$ (16)% ($a = 104$ d) or half that size in the period from mid 2004 to mid 2005 (with laboratory temperatures within 18.6 °C–22.9 °C). In this context, publication of a failure report is instructive.

4.3. *^{241}Am @SCK*

The γ-ray spectrometry service of the SCK•CEN (Belgium) provided 8 data sets of quality control measurements of a mixed ^{241}Am–^{152}Eu source on HPGe spectrometers #8, 10, 11, 13, 16, 25, 26, 27 between 2008 and 2016. The background- and decay-corrected area of the 59 keV peak for each detector (see e.g. figure 46 for detector #10) shows a quasi-linearly increasing trend with time and a jump in 2011 due to a change in data acquisition system [79]. The trend probably results from uncompensated count loss by pulse pileup

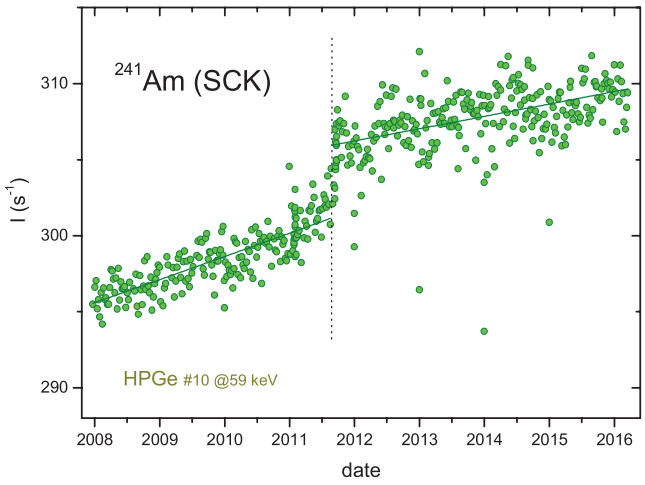

Figure 46. Decay-corrected net peak count rates at 59 keV from the decay of ^{241}Am measured with HPGe detector #10 at the SCK•CEN. The dotted line marks a change of data acquisition system and the full lines represent linear trend lines.

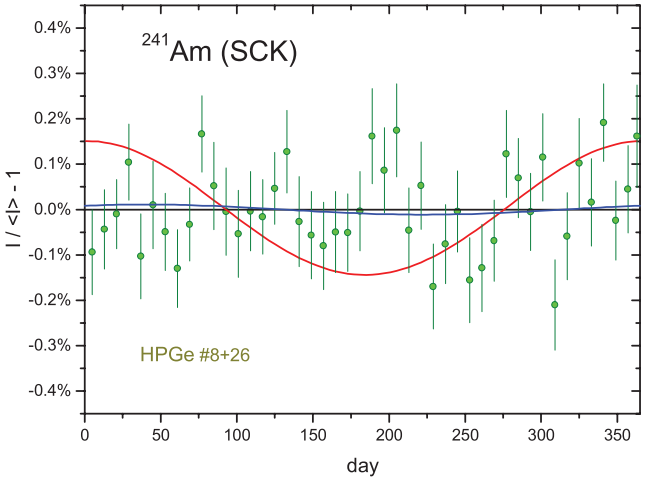

Figure 47. Annual average residuals from exponential decay for ^{241}Am activity measurements with HPGe-ray spectrometers #8 and #26 at SCK•CEN.

[80]. The data groups have been linearised and connected by means of the fit of two slopes and a scaling factor. The residuals have varying statistical accuracy, mainly depending on the detection efficiency at 59 keV, and also the stability for annual oscillations is largely different from one detector to another. Three groups of results were averaged: two detectors showing no annual effects in figure 47 ($A = 0.011$ (20)%, $a = 51$ d), three detectors with intermediately sized oscillations in figure 48 ($A = 0.065$ (13)%, $a = 255$ d), and three with large oscillations in figure 49 ($A = 0.139$ (20)%, $a = 244$ d).

The amplitudes (and phases) of the oscillation effects in each detector are almost identical for the ^{152}Eu data (see part III [59]), as can be verified in figure 50. They are mostly likely caused by seasonal effects on the detection efficiency, possibly through temperature effects on the geometry and electronics. One can exclude an explanation through changes in the decay constants in correlation with Earth–Sun distance,

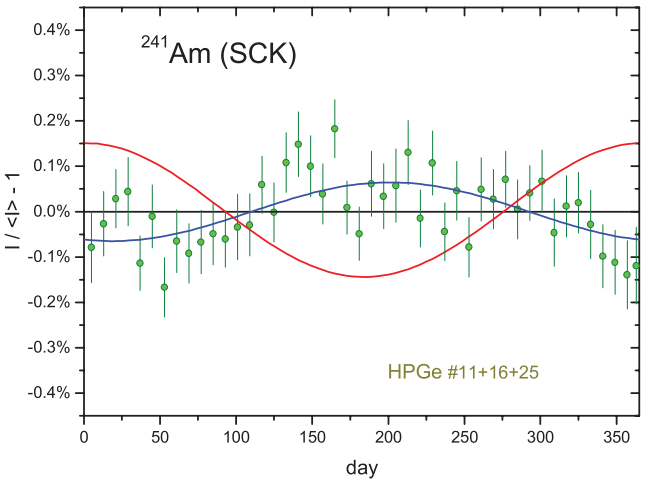

Figure 48. Annual average residuals from exponential decay for ^{241}Am activity measurements with HPGe-ray spectrometers #11, #16 and #25 at SCK•CEN.

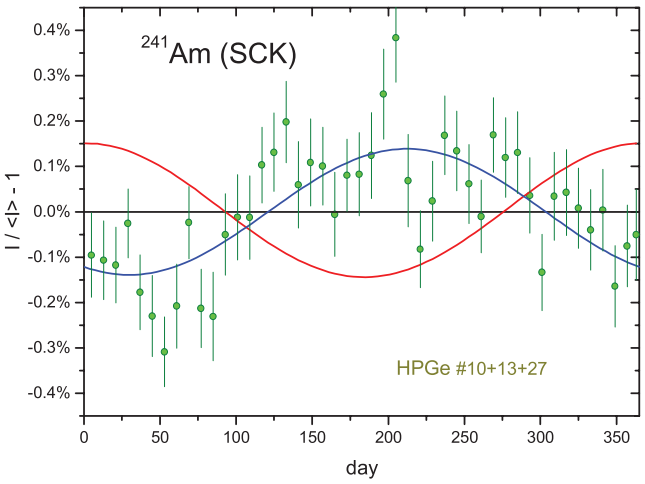

Figure 49. Annual average residuals from exponential decay for ^{241}Am activity measurements with HPGe-ray spectrometers #10, #13 and #27 at SCK•CEN.

because the most stable data sets confirm the invariability of the ^{241}Am decay constant down to sub-permille level.

4.4. ^{241}Am @PTB

At the PTB, 704 decay rate measurements were performed between 2014 and 2016 by means of a commercial TriCarb 2810 TR liquid scintillation counter. Two ^{241}Am and one background sample were prepared with Ultima Gold AB and water in glass vials. The duration of individual measurements was 12 h in all cases. The net counting rate was about 1200 s^{-1} and the relative statistical uncertainty was about 0.014%. One outlier (December 2014) was removed from the data sets. The background- and decay-corrected count rates show a slightly negative slope with time (figure 51). A possible explanation for this trend could be sample instability due to slight colour quenching [81]. Rate-related nonlinearity of the counter is less plausible considering that the counting rates did not vary much due to the long half-life of ^{241}Am. After having applied a linear correction, the average

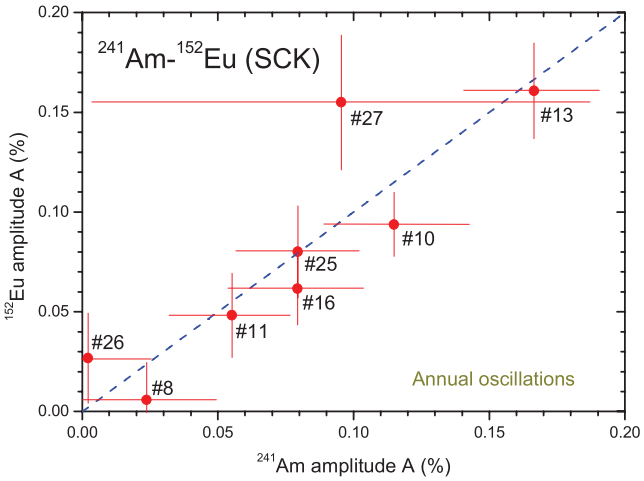

Figure 50. Amplitude of average annual oscillations in the decay rate of ^{241}Am and ^{152}Eu measured by γ-ray spectrometry with 8 detectors at SCK between 2008 and 2016.

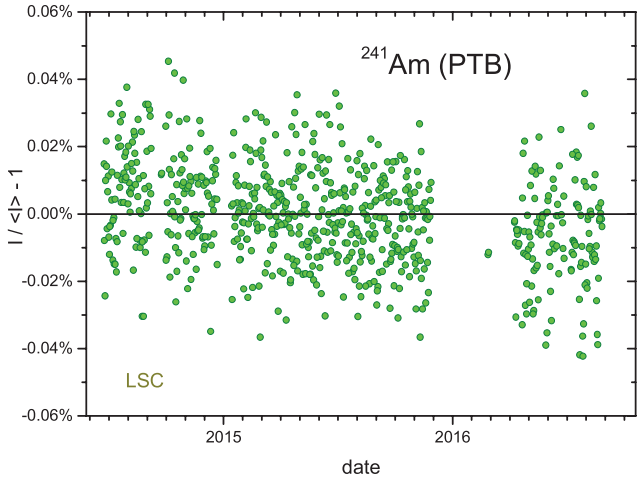

Figure 51. Residuals from exponential decay for ^{241}Am activity measurements with a liquid scintillation counter (LSC) at PTB.

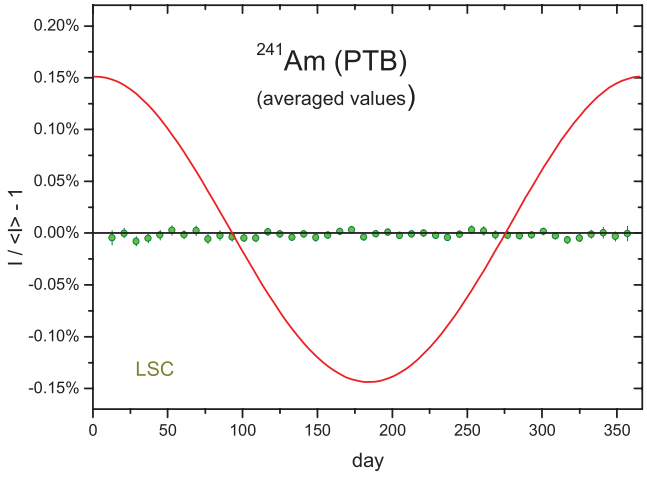

Figure 52. Annual average residuals from exponential decay for ^{241}Am activity measurements with a liquid scintillation counter (LSC) at PTB.

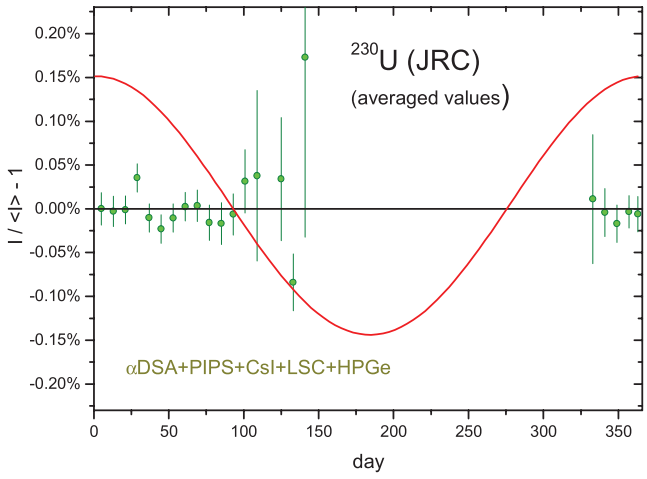

Figure 53. Annual average residuals from exponential decay for ^{230}U activity measurements with 5 different detectors at the JRC.

residuals in figure 52 show exceptional stability proving invariability of the decay constant down to the 10^{-6} level ($A = 0.0001\ (6)\%$, $a = 324$ d).

5. Uranium-230

5.1. Decay characteristics

Uranium-230 is a pure alpha emitter with a half-life of 20.23 (2) d [82] and its decay chain continues through a subsequent cascade of four alpha-emitting daughter nuclides with relatively short half-lives ranging between 30.70 (3) min (^{226}Th) and 164.2 (6) µs (^{214}Po) [83, 84]. It then proceeds through the long-lived beta emitter ^{210}Pb (22.23 (12) a), predominantly followed by another beta emitter (^{210}Bi) and an alpha emitter (^{210}Po).

5.2. ^{230}U @JRC

At the JRC, the decay of ^{230}U has been followed between November 2010 and mid 2011 with 5 detectors [82] (PIPS© alpha particle counter at defined solid angle, liquid scintillation counter, CsI sandwich spectrometer, HPGe γ-spectrometer, and PIPS© in 2π geometry [29]). The residuals to the exponential fits for parent and daughter nuclides have been published [82]. The averaged residuals over a period of nearly 200 d in figure 53 (excluding data affected by the ingrowth of the daughter products) show stability at a sub-permille level ($A = 0.007\ (7)\%$, $a = 173$ d). Since not a full year was covered, one could argue that oscillation effects may have been partly obscured by fitting the best matching exponential function, but the presence of annual oscillations at a permille level can be excluded.

6. Thorium-228

6.1. Decay characteristics

Thorium-228 ($T_{1/2} = 1.9126\ (9)$ a) decays 100% by alpha emission to ^{224}Ra (3.631 (2) d). The main alpha emission energy is at 5.4 MeV. The ^{228}Th decay can also be measured through characteristic γ rays of ^{224}Ra at 84 keV, 216 keV and some less intense peaks at higher energies.

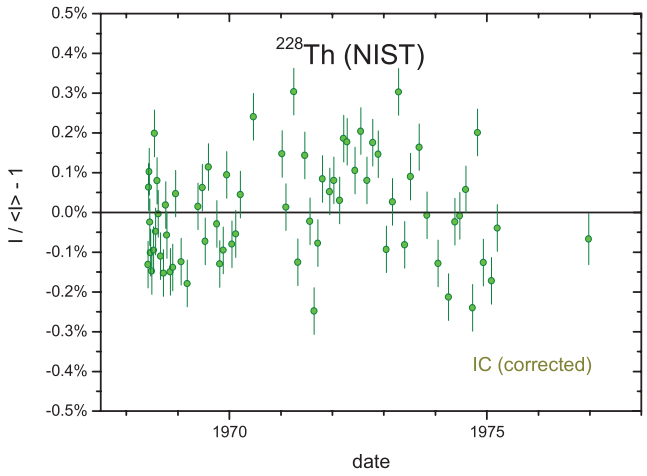

Figure 54. Annual average residuals from exponential decay for ^{228}Th decay rate measurements with IC 'A' at NIST, after minor corrections for geometrical instability of the source holder.

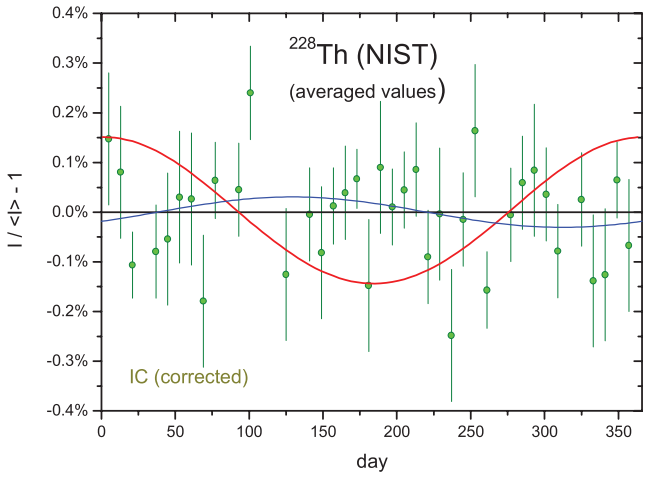

Figure 55. Annual average residuals from exponential decay for ^{228}Th decay rate measurements with IC 'A' at NIST, after minor corrections for geometrical instability of the source holder.

6.2. ^{228}Th @NIST

At the NIST, the decay of a ^{228}Th source has been measured in IC 'A' 70 times between 1968 and 1978 [85]. Smoothly varying correction factors (<0.03%) were applied to compensate for geometrical instability of the source holder [86], which explains some remaining auto-correlation effects in the residuals of figure 54. In spite of the slight trending, the average of the residuals (figure 55) show absence of annual oscillations at permille level ($A = 0.031$ (22)%, $a = 327$ d).

7. Conclusions

The ^{226}Ra decay curves from different laboratories show differences in stability which are uncorrelated in amplitude or time, but are strongly dependent on source activity and changes in the measurement set-up. The observed oscillations in the decay rates are not in phase with Earth–Sun distance, nor mutually coherent. Instability in the instrument and its local environment are the most plausible root cause of the variation of the detector signals. On an annual time scale, the decay curves show no obvious synchronous perturbations that could hint to influence from cosmic events. The most stable measurements confirm that the alpha decay of ^{226}Ra is purely exponential: if annual modulations of the ^{226}Ra decay constants exist, their amplitude must be less than $A = 0.0025$ (18)%. The ^{209}Po, ^{241}Am and ^{230}U decay constants are stable within $A < 0.01$% and ^{228}Th within 0.03%.

Acknowledgments

The authors thank all past and present colleagues who contributed directly or indirectly to the vast data collection over different periods spanning six decades. They are particularly indebted to Michael Unterweger, Ryan Fitzgerald, Denis Bergeron and Leticia Pibida of the National Institute of Standards and Technology (NIST, USA) for generously providing data sets for various nuclides.

Disclaimer

Certain commercial equipment is identified in this paper to foster understanding. Such identification does not imply recommendation or endorsement by the participating laboratories, nor does it imply that the materials or equipment identified are necessarily the best available for the purpose.

References

[1] Semkow T M 2007 Exponential decay law and nuclear statistics *Applied Modeling and Computations in Nuclear Science* (*ACS Symposium Series* vol 945) ed T M Semkow *et al* (Washington, DC: ACS/OUP) pp 42–56
[2] Pommé S 2015 The uncertainty of the half-life *Metrologia* **52** S51–65
[3] Emery G T 1972 Perturbation of nuclear decay rates *Annu. Rev. Nucl. Sci.* **22** 165–202
[4] Hahn H-P, Born H-J and Kim J I 1976 Survey on the rate perturbation of nuclear decay *Radiochim. Acta* **23** 23–37
[5] Bateman H 1910 The solution of a system of differential equations occurring in the theory of radio-active transformations *Proc. Camb. Phil. Soc.* **15** 423–7
[6] Pommé S *et al* 1996 General activation and decay formulas and their application in neutron activation analysis with k_0 standardization *Anal. Chem.* **68** 4326–34
[7] Arnold J R and Libby W F 1949 Age determinations by radiocarbon content: checks with samples of known age *Science* **110** 678–80
[8] Begemann F *et al* 2001 *Geochim. Cosmochim. Acta* **65** 111–21
[9] Pommé S, Jerome S M and Venchiarutti C 2014 Uncertainty propagation in nuclear forensics *Appl. Radiat. Isot.* **89** 58–64
[10] Pommé S and Collins S 2014 Unbiased equations for ^{95}Zr–^{95}Nb chronometry *Appl. Radiat. Isot.* **90** 234–40
[11] Pommé S, Collins S M, Harms A and Jerome S M 2016 Fundamental uncertainty equations for nuclear dating applied to the ^{140}Ba–^{140}La and ^{227}Th–^{223}Ra chronometers *J. Environ. Radioact.* **162** 358–70
[12] Nir-El Y *et al* 2007 Precision measurement of the decay rate of ^{7}Be in host materials *Phys. Rev.* C **75** 012801

[13] Litvinov Y A and Bosch F 2011 Beta decay of highly charged ions *Rep. Prog. Phys.* **74** 016301

[14] Atanasov D *et al* 2015 Between atomic and nuclear physics: radioactive decays of highly-charged ions *J. Phys. B: At. Mol. Opt. Phys.* **48** 144024

[15] Woods M J and Collins S M 2004 Half-life data—a critical review of TECDOC-619 update *Appl. Radiat. Isot.* **60** 257–62

[16] DDEP, 2004–2013. Table of radionuclides vol 1–7, monographie BIPM-5 BIPM, sèvres, website: www.nucleide.org/DDEP_WG/DDEPdata.htm

[17] Jenkins J H *et al* 2009 Evidence of correlations between nuclear decay rates and Earth–Sun distance *Astropart. Phys.* **32** 42–6

[18] Jenkins J H, Mundy D W and Fischbach E 2010 Analysis of environmental influences in nuclear half-life measurements exhibiting time-dependent decay rates *Nucl. Instrum. Methods.* A **620** 332–42

[19] Fischbach E *et al* 2009 Time-dependent nuclear decay parameters: new evidence for new forces? *Space Sci. Rev.* **145** 285–335

[20] Jenkins J H and Fischbach E 2009 Perturbation of nuclear decay rates during the solar flare of 2006 December 13 *Astropart. Phys.* **31** 407–11

[21] Mohsinally T, Fancher S, Czerny M, Fischbach E, Gruenwald J T, Heim J and Jenkins J H 2016 Evidence for correlations between fluctuations in ^{54}Mn decay rates and solar storms *Astropart. Phys.* **75** 29–37

[22] Jenkins J H *et al* 2013 Concerning the time dependence of the decay rate of ^{137}Cs *Appl. Radiat. Isot.* **74** 50–5

[23] Parkhomov A G J 2011 Deviations from beta radioactivity exponential drop *Mod. Phys.* **2** 1310–7

[24] Hardy J C *et al* 2010 Tests of nuclear half-lives as a function of the host medium and temperature: refutation of recent claims *Appl. Radiat. Isot.* **68** 1550–4

[25] Belloni F 2016 Alpha decay in electron environments of increasing density: from the bare nucleus to compressed matter *Eur. Phys. J.* A **52** 32

[26] Muir H 2006 Half-life heresy *New Sci.* **192** 36–9

[27] Mullins J 2009 Is the sun reaching into Earthly atoms? *New Sci.* **202** 42–5

[28] Clark S 2012 Half-life heresy: strange goings on at the heart of the atom *New Sci.* **216** 42–5

[29] Pommé S 2007 Methods for primary standardization of activity *Metrologia* **44** S17–26

[30] Simpson B and Judge S 2007 Special issue on radionuclide metrology *Metrologia* **44** S1–152

[31] Karam L, Keightley J and Los Arcos J M 2015 Special issue on uncertainties in radionuclide metrology *Metrologia* **52** S1–212

[32] Karam L and Ratel G 2016 Consultative committee on ionizing radiation: impact on radionuclide metrology *Appl. Radiat. Isot.* **109** 12–6

[33] Ratel G 2007 The Système International de référence and its application in key comparisons *Metrologia* **44** S7–16

[34] Pommé S 2006 An intuitive visualisation of intercomparison results applied to the KCDB *Appl. Radiat. Isot.* **64** 1158–1162

[35] Pommé S and Keightley J 2015 Determination of a reference value and its uncertainty through a power-moderated mean *Metrologia* **52** S200–12

[36] Pommé S 2016 When the model doesn't cover reality: examples from radionuclide metrology *Metrologia* **53** S55–64

[37] Lindstrom R 2016 Believable statements of uncertainty and believable science *J. Radioanal. Nucl. Chem.* (doi: 10.1007/s10967-016-4912-4)

[38] Norman E B *et al* 2009 Evidence against correlations between nuclear decay rates and Earth–Sun distance *Astropart. Phys.* **31** 135–7

[39] Bellotti E *et al* 2012 Search for time dependence of the ^{137}Cs decay constant *Phys. Lett.* B **710** 114–7

[40] Kossert K and Nähle O 2014 Long-term measurements of ^{36}Cl to investigate potential solar influence on the decay rate *Astropart. Phys.* **55** 33–6

[41] Bellotti E *et al* 2015 Search for time modulations in the decay rate of ^{40}K and ^{232}Th *Astropart. Phys.* **61** 82–7

[42] Nähle O and Kossert K 2015 Comment on 'Comparative study of beta-decay data for eight nuclides measured at the Physikalisch–TechnischeBundesanstalt'(2014 *Astropart. Phys.* **59** 47–58) *Astropart. Phys.* **66** 8–10

[43] Kossert K and Nähle O 2015 Disproof of solar influence on the decay rates of ^{90}Sr/^{90}Y *Astropart. Phys.* **69** 18–23

[44] García-Toraño E *et al* 2016 Standardisation and precise determination of the half-life of ^{44}Sc *Appl. Radiat. Isot.* **109** 314–8

[45] Novković D *et al* 2006 Testing the exponential decay law of gold ^{198}Au *Nucl. Instrum. Methods* A **566** 477–80

[46] Hardy J C, Goodwin J R and Iacob V E 2012 Do radioactive half-lives vary with the Earth-to-Sun distance? *Appl. Radiat. Isot.* **70** 1931–3

[47] Bellotti E *et al* 2015 Precise measurement of the ^{222}Rn half-life: a probe to monitor the stability of radioactivity *Phys. Lett.* B **743** 526–30

[48] Marouli M *et al* 2013 Decay data measurements on ^{213}Bi using recoil atoms *Appl. Radiat. Isot.* **74** 123–7

[49] Suliman G *et al* 2013 Half-lives of ^{221}Fr, ^{217}At, ^{213}Bi, ^{213}Po and ^{209}Pb from the ^{225}Ac decay series *Appl. Radiat. Isot.* **77** 32–7

[50] Bellotti E *et al* 2013 Search for correlations between solar flares and decay rate of radioactive nuclei *Phys. Lett.* B **720** 116–9

[51] Lindstrom R M *et al* 2011 Absence of a self-induced decay effect in ^{198}Au *Nucl. Instrum. Methods* A **659** 269–71
Lindstrom R M *et al* 2012 Absence of a self-induced decay effect in ^{198}Au *Nucl. Instrum. Methods* A **664** 231 (erratum)

[52] de Meijer R J, Blaauw M and Smit F D 2011 No evidence for antineutrinos significantly influencing exponential β^+ decay *Appl. Radiat. Isot.* **69** 320–6

[53] Barnes V E *et al* 2016 Search for perturbations of nuclear decay rates induced by reactor electron antineutrinos arXiv:1606.09325

[54] Meier M M M and Wieler R 2014 No evidence for a decrease of nuclear decay rates with increasing heliocentric distance based on radiochronology of meteorites *Astropart. Phys.* **55** 63–75

[55] Cooper P S 2009 Searching for modifications to the exponential radioactive decay law with the Cassini spacecraft*Astropart. Phys.* **31** 267–9

[56] Krause D E *et al* 2012 Searches for solar-influenced radioactive decay anomalies using spacecraft RTGs *Astropart. Phys.* **36** 51–6

[57] Pierre S *et al* 2010 On the variation of the ^{210}Po half-life at low temperature *Appl. Radiat. Isot.* **68** 1467–70

[58] Pommé S *et al* On decay constants and orbital distance to the Sun—part II: beta minus decay *Metrologia* **54** 19–35

[59] Pommé S *et al* On decay constants and orbital distance to the Sun—part III: beta plus and electron capture decay *Metrologia* **54** 36–50

[60] Pommé S *et al* Evidence against solar influence on decay constants *Phys. Lett.* B **761** 281–6

[61] Schrader H 2007 Ionization chambers *Metrologia* **44** S53–66

[62] Siegert H, Schrader H and Schötzig U 1998 Half-life measurements of europium radionuclides and the long-term stability of detectors *Appl. Radiat. Isot.* **49** 1397–401

[63] Schrader H 2004 Half-life measurements with ionization chambers—a study of systematic effects and results *Appl. Radiat. Isot.* **60** 317–23

[64] Schrader H 2010 Half-life measurements of long-lived radionuclides—new data analysis and systematic effects *Appl. Radiat. Isot.* **68** 1583–90
[65] Schrader H 2016 Seasonal variations of decay rate measurement data and their interpretation *Appl. Radiat. Isot.* **114** 202–13
[66] Javorsek D *et al* 2010 Power spectrum analyses of nuclear decay rates *Astropart. Phys.* **34** 173–8
[67] Sturrock P A *et al* 2014 Comparative study of beta-decay data for eight nuclides measured at the Physikalisch–TechnischeBundesanstalt *Astropart. Phys.* **59** 47–58
[68] Sturrock P A *et al* 2016 Analysis of beta-decay data acquired at the Physikalisch–Technische Bundesanstalt: evidence of a solar influence *Astropart. Phys.* **84** 8–14
[69] Goddard B *et al* 2016 Experimental setup and commissioning baseline study in search of time-variations in beta-decay half-lives *Nucl. Instrum. Methods* A **812** 60–7
[70] https://weatherspark.com/averages/28660/Brunswick-Niedersachsen-Germany
[71] Semkow T M 2009 Oscillations in radioactive exponential decay *Phys. Lett.* B **675** 415–9
[72] Hayashi K *et al* 2015 Normal seasonal variations for atmospheric radon concentration: a sinusoidal model *J. Environ. Radioact.* **139** 149–53
[73] Paepen J *et al* 2010 Half-life measurement of ^{124}Sb *Appl. Radiat. Isot.* **68** 1555–60
[74] Fitzgerald R P 2009 An automated ionization chamber for secondary radioactivity standards *Appl. Radiat. Isot.* **68** 1507–9
[75] Fitzgerald R *et al* 2014 A new NIST primary standardization of ^{18}F *Appl. Radiat. Isot.* **85** 77–84
[76] Pommé S and Benedik L 2016 *J. Radioanal. Nucl. Chem.* **309** 931–40
[77] Pommé S 2015 The uncertainty of counting at a defined solid angle *Metrologia* **52** S73–85
[78] Van Ammel R, Pommé S and Sibbens G 2006 Half-life measurement of ^{55}Fe *Appl. Radiat. Isot.* **64** 1412–6
[79] Bruggeman M, Verheyen L and Vidmar T 2014 A dedicated LIMS for routine gamma-ray spectrometry *Appl. Radiat. Isot.* **87** 425–8
[80] Pommé S, Fitzgerald R and Keightley J 2015 Uncertainty of nuclear counting *Metrologia* **52** S3–17
[81] Kossert K *et al* 2015 Uncertainty determination for activity measurements by means of the TDCR method and the CIEMAT/NIST efficiency tracing technique *Metrologia* **52** S172–90
[82] Pommé S *et al* 2012 Measurement of the ^{230}U half-life *Appl. Radiat. Isot.* **70** 1900–6
[83] Suliman G *et al* 2012 Measurements of the half-life of ^{214}Po and ^{218}Rn using digital electronics *Appl. Radiat. Isot.* **70** 1907–12
[84] Pommé S *et al* 2012 Measurement of the ^{226}Th and ^{222}Ra half-lives *Appl. Radiat. Isot.* **70** 1913–8
[85] Unterweger M P and Fitzgerald 2014 Update of NIST half-life results corrected for ionization chamber source-holder instability *Appl. Radiat. Isot.* **87** 92–4
[86] Fitzgerald R 2012 NIST Ionization chamber'A' sample-height corrections *J. Res. Natl Inst. Stand. Technol.* **117** 80–95